



**Please cite the Published Version**

Ekpo, Sunday Cookey , Elias, Fanuel, Uko, Mfonobong Charles, Sunday, Enahoro, Stephen, Alabi, Ijaz, Muhammad  and Unnikrishnan, Rahul (2025) Multi-Mode Multi-Source Electrical Power Subsystem Design for CubeSats-Internet of Things Missions. IEEE Access, 13. pp. 164965-164984.

**DOI:** <https://doi.org/10.1109/ACCESS.2025.3612339>

**Publisher:** IEEE

**Version:** Published Version

**Downloaded from:** <https://e-space.mmu.ac.uk/641885/>

**Usage rights:**  [Creative Commons: Attribution 4.0](https://creativecommons.org/licenses/by/4.0/)

**Additional Information:** This is an open access article published in IEEE Access.

**Enquiries:**

If you have questions about this document, contact [openresearch@mmu.ac.uk](mailto:openresearch@mmu.ac.uk). Please include the URL of the record in e-space. If you believe that your, or a third party's rights have been compromised through this document please see our Take Down policy (available from <https://www.mmu.ac.uk/library/using-the-library/policies-and-guidelines>)

Date of publication xxxx 00, 0000, date of current version xxxx 00, 0000.

Digital Object Identifier 10.1109/ACCESS.2024.0429000

# Multi-Mode Multi-Source Electrical Power Subsystem Design for CubeSats-Internet of Things Missions

**SUNDAY C. EKPO<sup>1</sup>, (Senior Member, IEEE), FANUEL ELIAS<sup>1</sup>, (Student Member, IEEE), MFONOBONG C. UKO<sup>1</sup>, (Member, IEEE), SUNDAY ENAHORO<sup>1</sup>, (Student Member, IEEE), STEPHEN ALABI<sup>2</sup>, MUHAMMAD IJAZ<sup>1</sup>, (Member, IEEE), RAHUL UNNIKRISHNAN<sup>2</sup> and NURUDEEN OLASUNKANMI<sup>2</sup>**

<sup>1</sup>Communication and Space Systems Engineering Team, Manchester Metropolitan University, Manchester, M15 6BH, UK. (e-mail: S.ekpo@mmu.ac.uk; Fanuel.Elias@stu.mmu.ac.uk; mfonobong.uko@stu.mmu.ac.uk; Sunday.Enahoro@stu.mmu.ac.uk; m.ijaz@mmu.ac.uk).

<sup>2</sup>SmOp Cleantech, Manchester, M40 8WN, UK. (e-mail: stephen.alabi@smopct.com; rahul.unnikrishnan@mmu.ac.uk; kolawole@smopct.com)

Corresponding author: Fanuel Elias (e-mail: Fanuel.Elias@stu.mmu.ac.uk).

This work was supported by the UKRI Funding Grant KTP13582/WT1261248.

**ABSTRACT** The need to extend the global coverage of mobile communication operators in 100 percent of the earth has accelerated the launches of 5G narrowband (NB)-internet of things (IoTs) non-terrestrial network (NTN) constellations of low-earth orbit (LEO) nanosatellites. Space-borne low-power IoTs sensors are power-hungry at highly variable rates during mission operations. The total energy reserve of the CubeSat-IoTs system is 24 hours premium resource constrained by the small satellite's solar eclipse regime(s). With the conventional heavy and rigid silicon-based solar technology design reaching its efficiency, use cases, and application limits, perovskite photovoltaic (PPV) solar cells have emerged as a worthy alternative. PPV's flexible and lightweight properties, cost-effective silicon panels' efficiency-boosting capability, and comparably cheaper production cost have attracted substantial commercial and scientific interests worldwide. To eliminate this problem, we propose a hybrid multiband radio frequency-perovskite photovoltaic energy harvester to sustain the constellation and/or clusters of CubeSat-IoTs systems operations anytime, anywhere, and optimise power supply equipment sizing and thermal reliability evaluation. This paper presents a multi-source multimode radio frequency-perovskite photovoltaic energy harvester development at the conceptual design phase of a CubeSat mission. This is supported by an experimental measurement of the actual power consumption of a field programmable gates array (FPGA) device in a typical CubeSat mission's digital design implementation. The power estimate is as close to the value obtained at the system integration phase. The results show that the FPGA device's quiescent (static) power consumptions at 50 and 100 MHz are 78 mW and 79 mW, respectively. Hybrid adaptive beamformed massive multiple-input-multiple-output heterogeneous cellular network (mMIMO-HetNets) green energy transmission and harvesting promise to address the small form factor (size, weight, power and cost) requirements and/or constraints of future sustainable small satellite missions in the LEO. The energy efficiency savings of the proposed multimode multiband RF-PPV energy harvesting and transmission system for the METCubeSat-IoTs mission is 0.23 Gb/J. This has enabled an energy budget balance for the operational space-borne devices with a multi-source N-power mode of operation to be developed for green 5G/6G/Wi-Fi and future-generation satellite-cellular convergence ecosystem and CubeSat-IoTs missions.

**INDEX TERMS** Adaptive devices, CubeSat mission, Energy harvesting, Electrical power subsystem, IoT sensors.

## I. INTRODUCTION

**L**OW power internet of things (IoTs) devices associated with the small satellites (e.g., CubeSats) utilise power at highly fluctuating rates, from picoamperes to amperes, and

from microseconds to seconds. Accurate in-orbit battery utilisation measurements are crucial to achieving the lengthy battery life for CubeSat-IoTs missions' success and/or potential

post-mission reuse. It is not sufficient for an in-orbit CubeSat-IoT device to have a short mission between impracticable battery replenishments [1]–[5]. Currently, in-orbit CubeSat-IoTs devices that last for the mission use case and/or application lifetime (typically well beyond a decade) are favoured. Chipset designers develop integrated electronic circuits with near-passive modes of operation that consume negligible current to satisfy decade-plus lifetime expectations. These IoTs devices typically operate with modes reduced instruction sets, slow clock speeds, and reduced current consumption, and battery voltages [5]–[9]. Wireless communications generally consume relatively large power. Hence, standards groups define new low-energy operating modes that combine simple connection protocols and low RF power levels for a limited active operational times mode. Wireless subsystems manufacturers design and test programmes for integrated processors to reduce power-consuming rates to extend the battery life [7]–[12].

The global supply chain of the electronics industry is in the top eight sectors, generating over 50% of the global carbon footprint. Physics-based effects of solar-activity-driven phenomena pose surmountable challenges to making CubeSat-IoTs clusters energy self-sufficient. Sustainable modular design and additive manufacturing can enable CubeSat-IoTs' surface and onboard electronics to be radiation-hardened against damaging space weather phenomena such as electromagnetic emissions and energetic particles [13], [14]. Besides the need for a high RF-to-direct current (DC) efficiency active semiconductor diodes, their semiconductor lattice structure needs to be radiation-hardened against charge creation by high-energy particle bombardment [16], [17]. Moreover, electronics must be shielded from single event effects. Our hybrid printed electronics approach can reduce the environmental hotspot impact of electronics using sustainable green energy-harvesting metamaterials/metasurfaces and advanced in-orbit reusability, reconfigurability, and remanufacturing technologies.

The behaviour and electrical power consumption of the CubeSat-IoT's electronic peripherals [2]–[4], [7], [12], [18]–[23] must be validated to integrate communication, sensing, control, propulsion, beamforming, MIMO RF architecture frontend and processing components into a final space-grade small satellite system [14], [15]. This enables an extra firmware or software control over electrical power supplies, mixed-signal and analogue components, and RF and digital / digitised analogue subsystems [18]–[21]. As the CubeSat-IoT system goes into production, test equipment are required to utilise a simpler set of tests to verify proper device operation rapidly, reliably and cost-effectively [13], [24]–[29]. The system design engineer is challenged by the different system-level electrical power budget needs to establish the exact measurements with varying mission-critical contingencies at each stage of the CubeSat-IoT design process [29]–[34]. The CubeSat-IoTs' chip and module developers must determine the power needs under different operational regimes (including uplink, downlink), factors, (including specific base

station architecture and site) times and states [23]–[26], [35]. The module developer needs to carry out very similar fast measurements on the different chips and correlate them to the module firmware operations [35]–[38]. The CubeSat-IoTs system designer must validate the accurate overall electrical power consumption throughout the product's hardware and software development process within the acceptable temporal resolution [38]–[43]. The manufacturing test aims to qualify the correct operational margins of the device using a simpler set of electrical power consumption test equipment [19].

Hybrid wireless multimode multiband radio frequency-solar power is the fastest-growing leading renewable energy technology for satellite-cellular communication ecosystem due to green government policies, increasing industry-academia partnerships, emerging new use cases and applications, decarbonization, substantial investments, active research advancements, small form factor space-borne subsystems requirements, massive low-carbon IoTs devices deployments, and emerging autonomous low-altitude economy globally [13], [30], [37], [42], [44]. Sustainable additively manufactured electronic and nanoscale 3D printing solutions can achieve 94% less CO<sub>2</sub> (kg/iteration); 99% less waste (kg/iteration); 100% less water (l/iteration); 82% less chemicals (l/iteration); and 98% less materials (kg/iteration). The multi-source multimode multiband energy transmission and harvesting (3M-ETH) radio frequency-perovskite photovoltaic (RF-PPV) system integrates electromagnetic waves and solar energy sources to achieve the most flexible and scalable high throughput gains by smartly offloading deterministic energy intelligence signal data traffics between NTN and TN SCs. The proposed innovative clean hybrid RF-perovskite photovoltaic energy harvesting, storage, transmission, distribution and utilisation solutions will enable space-borne massive MIMO CubeSat-IoTs electronic and mechanical devices operations.

The leading contributions of this research are the development of a green energy budget balance estimating relationship and the multi-source N-power mode renewable energy harvester design for the operational space-borne green 5G/6G / future-generation satellite-cellular convergence and CubeSat-IoTs missions. The reported research findings will enable the establishment of converged terrestrial network (TN) and non-terrestrial network (NTN) to create an interoperable dense heterogeneous networks (HetNets). The obvious benefit are energy and spectrum utilizations maximization due to a per unit area decrease in cell size and increase in the number of integrated TN-NTN small cells. This promising approach will satisfy the simultaneous energy and information data signal traffics demands anticipated in the LEO-based future-generation communication network ecosystem (including the 5G/6G satellite-cellular TN-NTN convergence). The massive (m) MIMO HetNets provide an enhanced alternative performance to the mMIMO by decreasing the energy consumption per small cell (SC) access point (AP). The presented multi-source multimode multiband energy transmission, and harvesting (3M-ETH) algorithm, and system model will enable

integrated TN-NTN SCAPs to be opportunistically switched on/off respecting the prevailing on-demand energy and spectrum traffics. Consequently, the 3M-ETH radio frequency-perovskite photovoltaic (RF-PPV) system will achieve high throughput gains by smartly offloading energy and information data signal data traffics between NTN and TN SCs.

This paper is organized as follows. Section II explains the CubeSat-IoTs' electrical subsystem engineering estimating relationships and margins for the meteorology, and other mission applications. Section III details the simulation and measurements results and analyses for a MetCubeSat-IoTs mission. A green 5G/6G CubeSat-Drone network for Earth observation / remote sensing application is presented in section IV. Section V concludes the paper.

## II. CUBESAT-IOTS ELECTRICAL SUBSYSTEM ENGINEERING DESIGN

### A. ADAPTIVE MIMO RF POWER COMPONENTS

The field programmable gate array (FPGA) has been utilised for various mission capabilities within the space community [5], [27], [32], [45]–[47]. This is due to its capabilities for parallelism, remote partial reconfiguration, high speed data transmission, radiation-hardness, very high logic density, cost-effectiveness and real-time operations. Latest works in space applications of FPGAs have focused on advancing its capabilities (including reconfiguration) with attendant reductions in size, weight, cost and failure [19], [27], [48]–[51]. Moreover, a small footprint FPGA has been reported to offer a cost-effective custom solution with hardware flexibility for ultra-low-power applications [19], [27]. As the drive for ultra-low-power FPGA applications heightens, there is a corresponding need for a system-level capabilities assessment. There is therefore a need for a system engineering analysis of how FPGA impacts the power budget of small satellite systems that define the multi-mode multi-source electrical subsystem design for CubeSats-internet of things (IoTs) missions. A typical radiation-hardened standard FPGA device contains combinatorial (C) and sequential (S) logic modules. This analysis is based on the Actel's RH 1020 and RH 1280 devices with two-level metal epitaxial bulk CMOS technology, 0.8  $\mu\text{m}$  process and using antifuse technology. RH 1020 features only the C-modules while the RH1280 features both C- and S-modules. A typical RH 1280 has a total of 1232 logic modules (608 C-modules and 624 S-modules) [7], [11], [12]. The total power consumption of the FPGA increases as the number of switched modules employed for a given application increases. Thus, limiting the number of modules switched by an elegant code design could greatly reduce the size of the solar array required for the entire mission.

A statistical analysis method is utilised to validate the mass-based power estimating relationships for LEO CubeSats [11]. The development of a reliable power contingency for the total power consumption of an adaptive device technology (such as the FPGA) requires the assessment of its various power components. The four basic power components of the FPGA device are: (i) Static (or quiescent) power; (ii)

Dynamic power; (iii) Power-up (or in-rush) power; and (iv) Configuration power. The static power is relatively constant throughout the CubeSat's mission and lifecycle. The dynamic power component is a function of the mission application and adaptive device technology onboard the small satellite. Competing FPGA technologies include antifuse, flash and SRAM. The first two FPGA technologies offer a combined lower static and dynamic power consumption than the third one for a given process length. Moreover, the antifuse and flash technologies have no power-up or configuration power consumption. The configuration data of flash-based FPGA technology can be retained after a system shutdown. In this thesis, the flash-based FPGA technology is recommended for the HASS architecture. The actual FPGA design and utilisation also determine the power consumption; a similar design can yield a different power dissipation on different devices. The dynamic power consumption of a FPGA is largely influenced by the clock speed. However, the dynamic power can be prohibitively high depending on the running application. Hence, a reliable power margin is inevitable to ensure space mission assurance and sustainability.

The actual power,  $P_{actual}(W)$ , of the CubeSat system for a meteorological satellite (METSAT) mission is obtained based on the subsystems and contingency factor,  $C_f$ , [11] as:

$$P_{actual} = \frac{(a + b) \times (1.96 + 0.96 \cdot C_f)}{0.96} \quad (1)$$

where  $a$  is the static subsystem power ( $P_{static}$ ) (W), and  $b$ , the dynamic subsystem power ( $P_{dynamic}$ ) (W).

Equation (1) constitutes the beginning-of-life (BoL) power requirements of the METSAT mission. It is expressed as a function of the static and the dynamic subsystem powers and the contingency factor for the adaptive CubeSat system design. It reveals that given the measured subsystem and payload power consumptions in the laboratory, the power budget of the HASS system can be estimated with ease.

### B. N-MODE PEROVSKITE PHOTOVOLTAIC ENERGY HARVESTER

The CubeSat-IoTs system generates 0 W during a solar eclipse and relies on the onboard storage batteries to sustain the critical mission operations. Batteryless passive CubeSat-borne IoTs devices promise to achieve low-cost net zero missions with on-demand in-orbit green energy generation capabilities. This paper proposes a hybrid multiple-input multiple-output multiband RF-perovskite photovoltaic (PPV) energy harvesting system to sustain the constellation and/or clusters of CubeSat-IoTs systems operations anytime, anywhere.

The CubeSat-IoTs device's 24-hour PPV energy,  $E_o$ , is obtained as [13]:

$$E_o = P_{sp}(\tau_o - t_e) \quad (2)$$

where  $P_{sp}$  = the solar panel's daytime average sunlit power generation (W);  $\tau_o$  = orbital period or actual total operational

time (maximum = 1440 minutes) of the CubeSat-IoTs device(s); and  $t_e$  = eclipse time of the CubeSat.

A hybrid two-power mode MIMO energy harvesting CubeSat-IoTs system has a 24-hour period total energy profile defined by:

$$E_o = E_s + E_p \quad (3)$$

where  $E_s$  = CubeSat-IoTs system's power-storing mode's energy consumption (J); and  $E_p$  = the CubeSat-IoTs system's payload processing-overpower mode energy consumption (J). The in-orbit payload processing-overpower mode's operational time,  $t_p$ , [9] is obtained as:

$$t_p = \tau_o - (t_s + t_e) \quad (4)$$

where  $t_s$  is the power-storing mode time. From (2) and (3), a two-power mode system translates (4) into:

$$t_p = \frac{E_o - P_s(\tau_o - t_e)}{P_p - P_s} \quad (5)$$

Equation (5) can be adjusted to accommodate CubeSat-IoTs missions with a multi-source N-power modes of operation [9], [11], [13]. Hence, the active service operational time of the payload processing-overpower mode [9], [13] is:

$$t_p = \frac{E_o - P_s(\sum_{i=1}^{N-2} t_i + t_e - \tau_o) - (\sum_{i=1}^{N-2} P_i t_i)}{P_p - P_s} \quad (6)$$

where  $P_i$  = CubeSat-IoTs system's  $i_{th}$  power mode's power consumption; and  $t_i$  = CubeSat-IoTs system's  $i_{th}$  power mode's operational time.

### C. THE MULTIBAND N-MODE RF ENERGY HARVESTER

The multi-mode multiband RF energy harvesting estimating relationship is derived with the assumption that the gains of the CubeSat-IoTs system's transmit and receive antennas are non-reconfigurable and static. Mathematically, the multi-source N-power modes multiband MIMO RF energy harvesting function is given by thus:

$$P_{rT}(W) = \sum_0^n P_m(W) = \sum_0^i P_{t_{ni}} G_{t_n} \left( \frac{\lambda_{ni}}{4(\pi) R_{n-m}} \right)^2 G_{t_m} \quad (7)$$

where the parameters for transmitter  $n$  and receiver  $m$  are defined as:  $R_{n-m}$  = Distance of the transmitter  $n$  from the receiver  $m$  in metres;  $G_{t_n}$  = Static gain of the antenna of transmitter  $n$  in dB;  $G_{t_m}$  = Static gain of the antenna of transmitter  $m$  in dB;  $P_{rT}$  = Power received from transmitter  $n$  in Watt;  $P_{t_{ni}}$  = Power from frequency  $i$  of transmitter  $n$  in Watt;  $P_{rT}$  = Total Power received from all the transmitters in Watt;  $\lambda_{ni}$  = Wavelength of signal (frequency)  $i$  from transmitter  $n$  in metres.

### D. THE HYBRID MIMO MULTIBAND RF-PPV ENERGY HARVESTING SYSTEM MODEL

The LEO base station transmits RF signals through multiple channels characterized by a combination of line-of-sight (LOS) and non-line-of-sight (NLOS) paths. The entire uniform linear multiband multichannel MIMO array's received signal vector,  $S_r(t)$ , (Fig. 1) is obtained as follows:

$$S_r(t) = \sum_{i=1}^M x_i(t) \quad (8)$$

Each RF sensor's received signal,  $x_i(t)$ , is given by (9), where  $s_i(t)$  = received desired signal,  $n_i(t)$  = dynamic system noise.

$$x_i(t) = s_i(t) + n_i(t) \quad (9)$$

The constraint matrix [3], [12] of the RF-PPV system is obtained from the column vectors of length  $JM$  where  $M$  is RF antenna sensors, and  $J$  = FIR filter coefficients

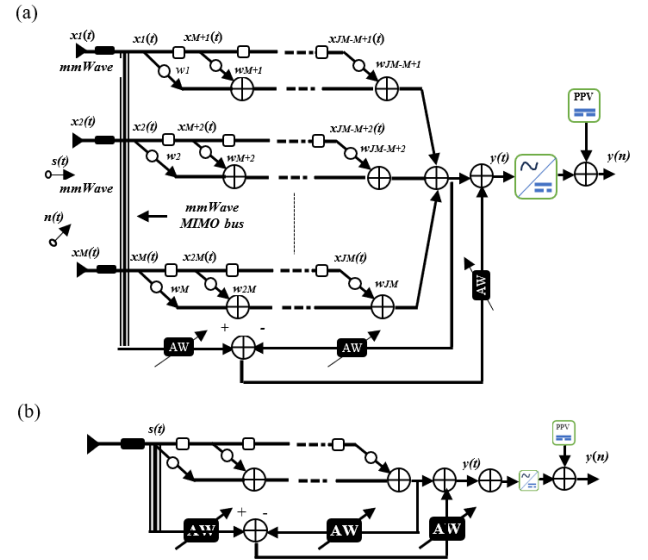


**FIGURE 1.** Hybrid MIMO Multiband RF-PPV Energy Harvesting System Model Architecture (a) Expanded version (b) Condensed version [3], [12]

The small coverage areas by TN-NTN small cells limit the quality of service and seamless ubiquitous connectivity offered to highly mobile IoTs devices [16], [52]–[54]. The proposed mMIMO-HetNets RF-PPV energy transmission and harvesting system model utilizes a two-tier CubeSat-IoTs network architecture with mMIMO macro cell tier ETH base stations (BSs) and HetNets small cell tier ETH pico, and femto cells. The CubeSat-IoTs mMIMO macro cell tier enables highly mobile IoTs devices with a uniform service coverage. The CubeSat-IoTs small cell tier supports localized clusters, constellations, indoors, and outdoors TN-NTN ETH beamforming capacity requirements [3], [12]. This elegant system architecture promises simultaneous real-time benefits of HetNets-enabled array gains and mMIMO-enabled multiplexing gains. For a 4-antenna multiband multichannel sub-6 GHz CubeSat-IoTs mission with 4 finite impulse response

taps, we consider the odd-numbered electromagnetic (EM) waves sensors to be 2.4 GHz band MIMO channels EM sensors and the even-numbered, 5.8 GHz [3], [12], [19]. A summary of the reconfigurable weight vectors,  $w$ , for green two-source, three-mode multiband RF energy harvesting and transmission operations in an interference-prone space environment is obtained as follows:

#### Mode 1: 2.4 GHz-PPV Energy Harvesting and Transmission Only

$$W_{2.4 \text{ GHz-PPV}} = \begin{bmatrix} w_1 & w_3 & \cdots & w_{M-1} \\ w_{M+1} & w_{M+3} & \cdots & w_{2M-1} \\ \vdots & \vdots & \ddots & \vdots \\ w_{JM-M+1} & w_{JM-M+3} & \cdots & w_{JM-1} \end{bmatrix} \quad (10)$$

The corresponding impulse response,  $f_{2.4 \text{ GHz-PPV}}$ , is thus:

$$f_{2.4 \text{ GHz-PPV}} = \begin{bmatrix} W_1 + W_3 \\ W_5 + W_7 \\ \vdots + \vdots \\ W_{13} + W_{15} \end{bmatrix} \quad (11)$$

#### Mode 2: 5.8 GHz-PPV Energy Harvesting and Transmission Only

$$W_{5.8 \text{ GHz-PPV}} = \begin{bmatrix} w_2 & w_4 & \cdots & w_M \\ w_{M+2} & w_{M+4} & \cdots & w_{2M} \\ \vdots & \vdots & \ddots & \vdots \\ w_{JM-M+2} & w_{JM-M+4} & \cdots & w_{JM} \end{bmatrix} \quad (12)$$

The corresponding impulse response,  $f_{5.8 \text{ GHz-PPV}}$ , is thus:

$$f_{5.8 \text{ GHz-PPV}} = \begin{bmatrix} W_2 + W_4 \\ W_6 + W_8 \\ \vdots + \vdots \\ W_{14} + W_{16} \end{bmatrix} \quad (13)$$

#### Mode 3: Simultaneous Multiband Multichannel Sub-6 GHz-PPV Energy Harvesting and Transmission

$$W_{\text{RF-PPV}} = \begin{bmatrix} w_1 & w_2 & \cdots & w_M \\ w_{M+1} & w_{M+2} & \cdots & w_{2M} \\ \vdots & \vdots & \ddots & \vdots \\ w_{JM-M+1} & w_{JM-M+2} & \cdots & w_{JM} \end{bmatrix} \quad (14)$$

The corresponding simultaneous N-mode multiband multichannel RF-PPV impulse response,  $f_h = [f_1, f_2, \dots, f_J]^T$  is thus:

$$f_1 = \sum_{i=1}^M w_i, \quad f_2 = \sum_{i=M+1}^{2M} w_i, \quad f_J = \sum_{i=JM-M+1}^{JM} w_i \quad (15)$$

We have designed the logic sequence for achieving reconfigurable simultaneous multimode multiband RF-PPV in a functional simulation. We assume that the FPGA fabric's interconnects and logic elements/blocks are perfect with zero

signal travel delays. This ascertains the design stage circuit's functional integrity with a low latency that uses the logic expressions to validate the digital circuit. The timing simulation considers the signal travel and tests the fitter circuit to validate its functional timing and correctness. RF-PPV Logic Sequence for RF1 (2.4 GHz) and RF2 (5.8 GHz) is explained thus:

#### Output:

- $y = 1$  (Receive/Transmit Energy Signal Data; Receiver (Rx) / Transmitter (Tx) for RF1-PPV / RF2-PPV; [Latency, Energy Signal Data Rate] = [High/Low, High/Low]).

#### Inputs:

- $x_3 = 1$  (Favorable Multichannel Conditions or Energy Signal Data Transmission Request Detected)
- $x_1 = 1$  (Transmit energy signal data using RF1-PPV)
- $x_2 = 0$  (Rx/Tx Shutdown)

#### Logic:

- The RF1-PPV MIMO Transceiver transmits energy signal data when unfavorable multichannel conditions are detected for RF2-PPV (low-to-medium latency and low-to-high energy signal data rate;  $x_1 = 1; x_2 = 0; x_3 = 0$ ).
- The RF2-PPV MIMO Transceiver transmits energy signal data when favorable multichannel conditions are detected for RF2-PPV (low latency and high data rate;  $x_1 = 0; x_2 = 0; x_3 = 1$ ).
- The hybrid multiband RF1-PPV–RF2-PPV MIMO transceiver transmits energy signal data when unfavorable (using RF1-PPV) or favorable channel (using RF2-PPV) conditions are detected for RF2-PPV (low-to-medium latency and low-to-high energy signal data rate;  $x_1 = 1; x_2 = 0; x_3 = 1$ ).

**TABLE 1.** Truth table for the digital hybrid RF1-PPV–RF2-PPV switching modes

$x_1$	$x_2$	$x_3$	$y$
0	0	0	0
0	0	1	1
0	1	0	0
0	1	1	0
1	0	0	1
1	0	1	1
1	1	0	0
1	1	1	0

Table 1 shows the truth table of the multimode multiband multichannel MIMO RF-PPV energy harvesting and transmission system with a 50% probability for both RF1-PPV and RF2-PPV channels to receive / transmit energy signal data. Hence, this achieves asynchronous energy signal data receptions and transmissions for multi-source multimode multiband multichannel variable latency and energy signal data rate requirements for autonomous CubeSat-IoTs communication use cases and/or applications. This promises to enable low-altitude-borne and space-based meshed mMIMO-IoTs

applications for variable-range ultra-low-latency spectrum- and energy-efficient autonomous inter-satellite, CubeSat-to-drone / air taxi, and satellite-to-earth stations communications [9], [11], [12], [19]. The presented RF-PPV system architecture and mathematical model utilises a FPGA-based truth table (Table 1) to switch between the three modes. The system simulation generates  $2^n$  test vectors for  $n$  mMIMO RF1-PPV and RF2-PPV inputs. Functional and timing simulations were carried out using the Quartus II Simulator. Fig. 2 shows the schematic digital circuit design implementing the three-input MIMO RF-PPV switching modes.

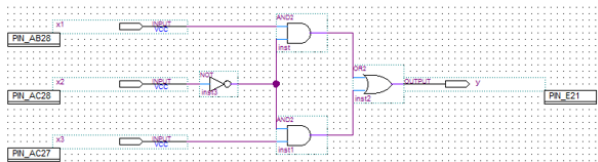


**FIGURE 2.** A Schematic Digital Design of the 3-Input RF-PPV Switching Modes.

Within the context of this paper, energy signal data rate is the speed of data transmission within a system that simultaneously manages multimode, multisource energy harvesting and consumption. It measures how much data can be transferred within a given time frame (latency), whilst also profiling the energy generation and usage of the process. Within the context of this paper, reconfigurable weight vectors (*RWV*) refer to the sets of reconfigurable beamforming values representing the core contributions to hybrid green multi-source, multi-mode multi-band RF-solar energy harvesting and transmission operations in an interference-prone space environment. *RWVs* quantify how much each contributing reconfigurable element of the source and/or mode and/or utilising duty cycle operation influences the total in-orbit real-time harvested green energy. The constrained system impulse response is the product of the constraint matrix, and the weight vectors. It is obtained as a dimensional vector of the sum of the weight vectors as revealed in (11), (13) and (15) [3], [12]. Within this context, the weight vectors are the scaling and combining coefficients of these impulse responses to model the complex hybrid multi-source, multi-mode energy harvesting system behavior or to combine multiple constrained system impulse responses.

The orbital patterns [9], [11], [19] must be carefully analysed to validate the operational times of capability-based CubeSat systems. The proposed hybrid RF-PPV energy transmission and harvesting model in a satellite-cellular HetNet-mMIMO connectivity convergence ecosystem considers two case studies for a LEO-based meteorology mission, viz: (i) Case study 1 = spacecraft team payload; and (ii) Case study 2 = customer-furnished payload.

### Case Study 1: Spacecraft Team Payload

$$P_T = 1.13M_{HAN} + \frac{P_{pl} + (1 + C_l)(1 - C_l)(P_e - P_{pl})}{2} + 1.72 \quad (16)$$

## Case Study 2: Customer-Furnished Payload

$$P_T = 1.13M_{HAN} + \frac{(1 + C_l)(1 - C_{lf})P_{pl}}{2} + 1.72 \quad (17)$$

Where;  $P_T$  = total in-orbit meteorology CubeSat-IoTs power requirements (W);  $M_{HAN}$  = mass of a highly adaptive CubeSat (kg);  $C_{lf}$  = cable loss factor;  $P_{pl}$  = payload power consumption (W);  $P_t$  = payload-based power estimating relationship (W).

The 5G/6G satellite-cellular convergence ecosystem is expected to enable peak data rates from 100 Gbps to 1 Tbps data throughput in the sub-THz radio access technology regime. This will provide a seamless and ubiquitous connectivity for a massive number of TN and NTN IoTs devices per unit area. With this potential huge low-power devices comes the critical need for autonomous on-demand green energy supply to limit and/or reduce the enormous carbon footprint contributions of the existing 5G networks [16], [52]–[55]. An essential energy budget design consideration for the converged 5G/6G NTN-TN networks is the energy efficiency (EE) in bit-per-joule. Mathematically, this is given by:

$$EE = \frac{R}{P} \quad (18)$$

where:  $R$  = system throughput (bit) and  $P$  = power consumed (W) to achieve  $R$ . We propose the mMIMO-HetNet technology as an enabler to achieve multiple orders of energy and spectral efficiency gains for the NTN-TN over the current radio access technologies implementations.

### III. SIMULATION AND MEASUREMENTS RESULTS AND ANALYSES FOR A METCUBESAT-IOTS MISSION

### A. METCUBESAT-IOTS MISSION ENERGY BUDGET ANALYSIS

This paper considers four payload subsystems at different altitudes and inclinations (Tables 2-5), viz:  $P1$  (387.6 mW),  $P2$  (717.6 mW),  $P3$  (257.6 mW) and  $P4$  (537.6 mW) for the METCubeSat-IoTs mission spanning a heterogeneous TN-NTN ecosystem with mMIMO SCAPs. The higher the camera's spatial resolution, the more the mission power requirement / consumption. The mechanical properties of the proposed METCubeSat-IoTs are thus: density = 1000 kg/m<sup>3</sup>; size: 21cm x 21 cm x 21 cm; and weight = 9.2 kg [9], [12]. The four payloads each has a 40-minute operational time at 180° inclination and 800 km altitude ( $H_{sat}$ ) [9]. More payload operational time enables high data integrity and quality. The excess energy stored for the candidate payload configurations during the METCubeSat-IoTs mission are presented in Figs. 3 ( $P1$ ), 4 ( $P2$ ), 5 ( $P3$ ), 6 ( $P4$ ). The sun-synchronous orbits lead in storing the highest amount of energy for each CubeSat payload configuration (Figs. 3 - 5). To achieve more operational times for the payload processing-overpower mode, a 3.99-Wh Li-ion battery can store the excess energy,  $E_{ep}$ , per round trip to sustain the mission and accommodate the eclipse time threshold. The excess energy stored for the candidate payload configurations versus the operational times during

the METCubeSat-IoTs mission are presented in Figs. 6 (P1), 7 (P2), 8 (P3), 9 (P4). The minimum-to-maximum storable excess energy ratio is 1:3.39 for the candidate METCubeSat-IoTs mission payloads. At a Sun-synchronous (polar) 90 orbit, the P2's excess energy storage is maximum at 4.81 Wh. This would accommodate more operational times and secondary payloads for the proposed METCubeSat-IoTs mission with two polymer Li-ion batteries (with a combined capacity of 7.78 Wh).

**TABLE 2.** Orbital assignments

Orbit	Number	$H_{sat}$ (km)
Equatorial	1	300
Inclination 22.5	2	400
Inclination 45	3	500
Inclination 67.5	4	600
Inclination 90 (polar)	5	300
Inclination 112.5	6	400
Inclination 135	7	500
Inclination 157.5	8	600
Inclination 180	9	800
Sun-synchronous (polar) 90	10	300
Sun-synchronous (nonpolar) 98	11	400

**TABLE 3.** Power budget of payload modules for the METCubeSat-IoTs mission [9]

Design Parameter	Payload Module			
	$P_1$	$P_2$	$P_3$	$P_4$
Payload module power, W	14.010	14.340	13.880	14.160
Core bus power, W	8.180	7.910	8.280	8.060
Power margin, W	2.040	1.980	2.070	2.010

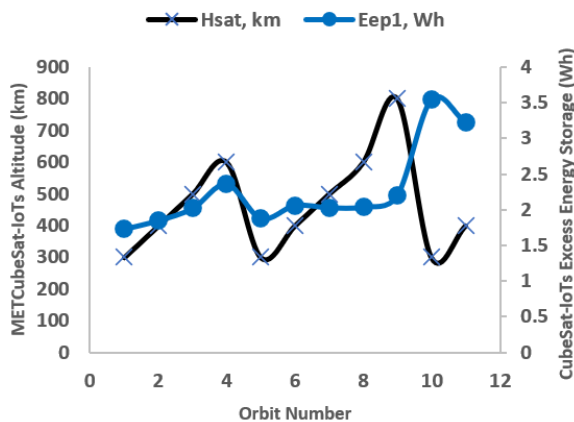


**FIGURE 3.** Altitude of METCubeSat-IoTs versus Excess Energy Storage of Payload 1

To demonstrate the significantly high energy efficiency of the proposed RF-PPV energy transmission and harvesting system in a mMIMO-HetNet for the NTN-TN convergence ecosystem, Table 6 shows Power budget for the METCubeSat-IoTs mission using payload P4 [9]. The uplink-overpower mode's power consumption is 750 mW. The authors have designed a LEO-based CubeSat-IoTs RF-PPV

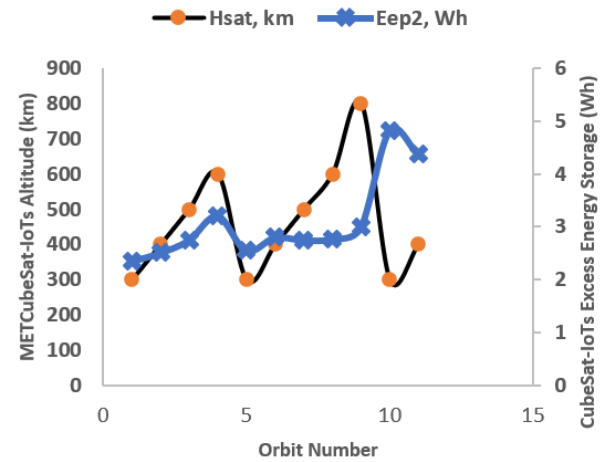


**FIGURE 4.** Altitude of METCubeSat-IoTs versus Excess Energy Storage of Payload 2

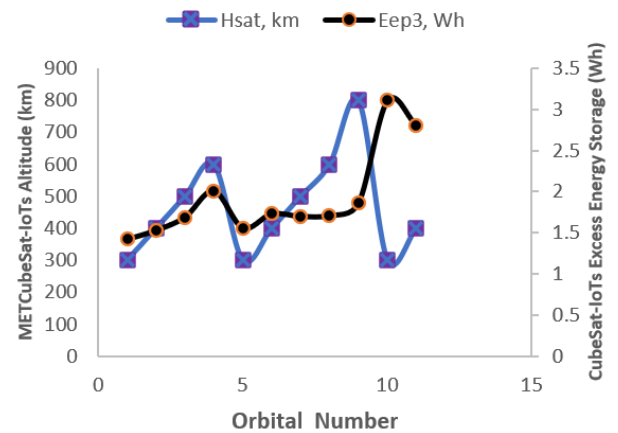


**FIGURE 5.** Altitude of METCubeSat-IoTs versus Excess Energy Storage of Payload 3

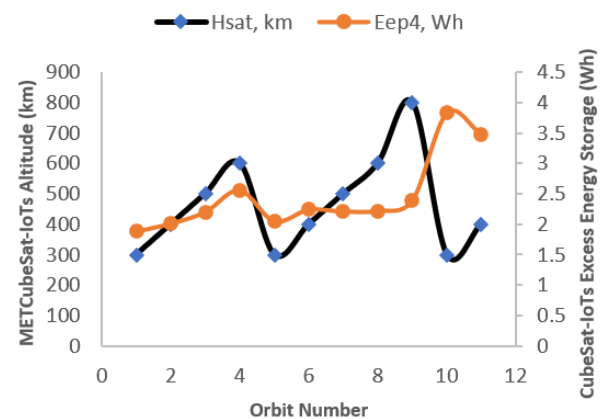


**FIGURE 6.** Altitude of METCubeSat-IoTs versus Excess Energy Storage of Payload 4

system that can generate 650 mW on-demand within the NTN-TN convergence ecosystem. Assuming a constant energy harvesting and intersatellite uplink data transmission, the

**TABLE 4.** Payloads 1 and 2 Subsystems Requirements for the METCubeSat-IoTs Mission [9]

Feature	Payload 1 (P1)	Payload 2 (P2)
Sensor technology	OmniVision 2655 CMOS image camera	Mitsubishi's CCD camera module
Sensor power consumption, mW	250	580
FPGA device	Spartan-3 XC3A400T	Spartan-3 XC3A400T
FPGA power Consumption, mW	137.6	137.6
Spatial resolution, pixel	2 x 1024 x 1024	1152 x 864 x 2
Spectral resolution, bit	3 x 8	3 x 8

**TABLE 5.** Payloads 3 and 4 subsystems requirements for the METCubeSat-IoTs mission [9]

Feature	Payload 3 (P3)	Payload 4 (P4)
Sensor technology	Sanyo's CCD camera module	Sharp's LZ0P373F CCD camera module
Sensor power consumption, mW	120	400
FPGA device	Spartan-3 XC3A400T	Spartan-3 XC3A400T
FPGA power Consumption, mW	137.6	137.6
Spatial resolution, pixel	1 x 1024 x 1024	1632 x 1224
Spectral resolution, bit	3 x 8	3 x 8

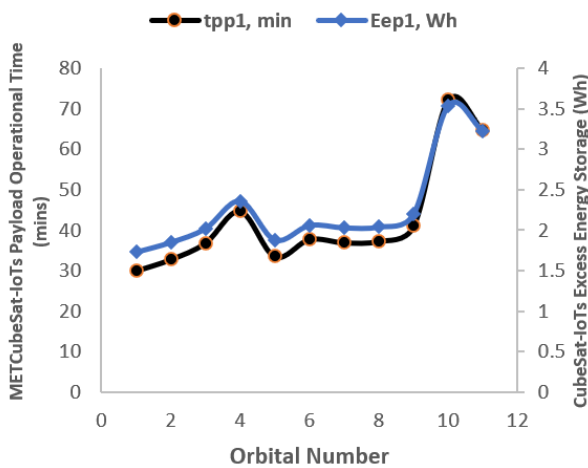


**FIGURE 7.** METCubeSat-IoTs Operational Time versus Excess Energy Storage of Payload 1

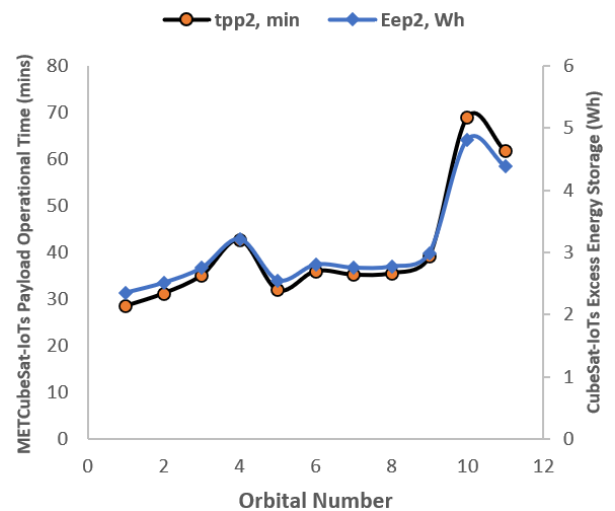


**FIGURE 8.** METCubeSat-IoTs Operational Time versus Excess Energy Storage of Payload 2

energy efficiency savings (EES) profile in Fig. 12 holds a great promise for the future-generation converged NTN-TN ecosystem. The analysis reveals that an EES of 0.23 Gb/J is achieved for the uplink data throughput.

The European Commission (2025) estimates that approximately 80% of an electronic product's environmental impact is created at the design stage. The RF-perovskite photovoltaic energy harvesting model applies economically efficient and environmentally friendly advanced nanoscale printed electronics and precision hybrid manufacturing technologies to convert digital designs into ubiquitous on-demand intelligent functioning products. Consequently, directed assembly-based printing is utilised to print circuits at the nano and

microscale to reduce components and carbon footprints. Our proposed sustainable RF-perovskite photovoltaic energy harvesting model enables early space-grade product's development process decisions to ensure its longevity, reconfigurability, reuse, repairability, recyclability, remanufacturability and end-of-life value inventory validation irrespective of the deployment altitude, orbital shadowing condition and space weather effects. A CubeSat-IoTs' orbit intersects the Earth's eclipse (or shadow) during its trajectory around the latter. This causes a reduction in solar energy radiation and affects the CubeSat-IoTs' power and thermal systems. The sustainable design and hybrid advanced manufacturing of

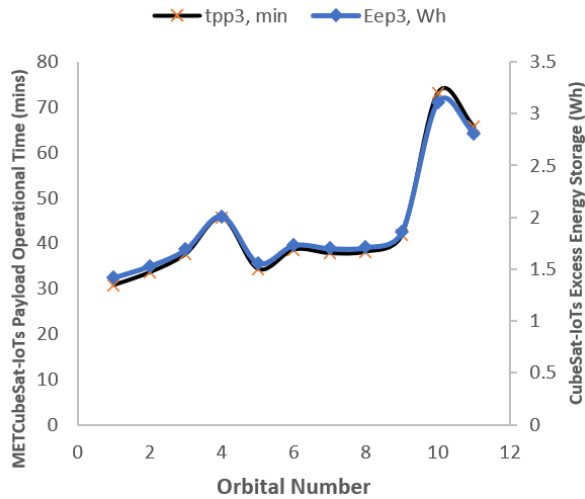


**FIGURE 9.** METCubeSat-IoTs Operational Time versus Excess Energy Storage of Payload 3

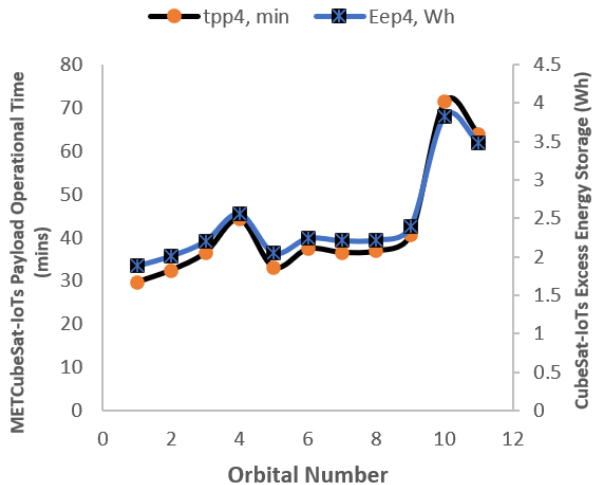


**FIGURE 10.** METCubeSat-IoTs Operational Time versus Excess Energy Storage of Payload 4

electronics (HAME) process of the proposed RF-PPV energy harvester obviates the operational consequences of the orbital shadowing (or eclipse) phenomenon when the Earth's full shadow (umbra) or partial shadow (penumbra) is crossed by the CubeSat-IoTs in LEO [15]. During orbital shadowing, the CubeSat-IoTs' solar panels are shielded from the sunlight, leading to a power generation decrease and the CubeSat's thermal environment changes. The proposed CubeSat-IoTs' power system (or RF-PPV energy harvester) is sustainably designed and manufactured to handle these periods of orbital shadowing (or decreased solar radiation) to activate / recharge the onboard batteries using sun-synchronous [polar ( $90^\circ$ ) or non-polar ( $98^\circ$ )] microsatellites at higher orbits to complement (or as) other backup sources. The RF-PPV model effectively preserves the CubeSat-IoTs performance and longevity by integrating accurate modelling of the orbital shadowing in mission planning and CubeSat-IoTs' electrical power sub-

system design. The shadow function parameter value range [i.e., 0 (no sunlight) - 1 (full sunlight)] is optimally chosen to scale the CubeSat-IoTs' location's solar radiation flux during orbital shadowing. With a sun-synchronous orbit deployment for a consistent sunlight angle relative to the sun, the CubeSat-IoTs spends a minimum time in the Earth's shadow (umbra or penumbra). Fig. 11 shows how the CubeSat-IoTs' altitude (km) varies with the orbit orbital inclination (deg) and the excess energy storage (Wh) for the proposed RF-PPV energy harvesting model.

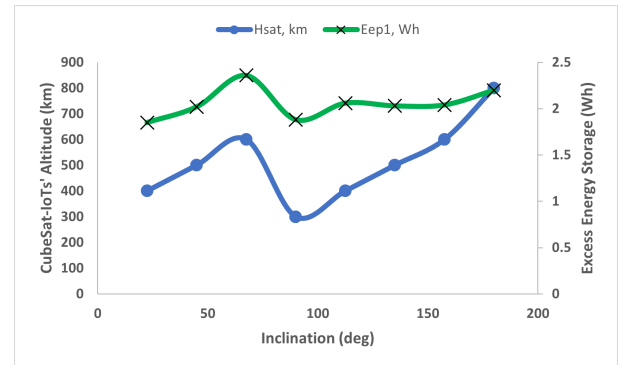


**FIGURE 11.** CubeSat-IoTs' RF-PPV Energy Harvester's Excess Energy for Payload 1 versus Orbital Inclinations at different Altitudes

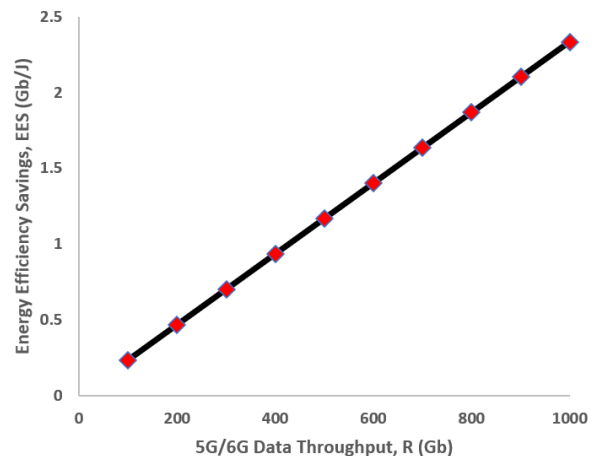


**FIGURE 12.** In-orbit Energy Efficiency Savings Profile METCubeSat-IoTs mission (P4)

## B. CUBESAT -IOTS POWER CONSUMPTION MODELING AND MEASUREMENTS

The FPGA power consumption measurement is a complex and difficult process and device manufacturers have provided power estimation tools for the prevailing design phases. The power consumption of a FPGA device is almost mainly dynamic. Hence, the digital design for a given application determines the FPGA power requirement. The FPGA power consumption is affected by the output loading, supply voltage, design density (number of interconnects), logic block and interconnect structure, system performance (switching

**TABLE 6.** Power budget for the METCubeSat-IoTs mission using payload P4 [9].

Subsystem	Power Mode's Power Consumption (W)			
	Power-storing	Communication-overpower (W)	Uplink-overpower (W)	Payload processing-overpower (W)
ADC	0	0	0	0
C&DH	2.500	2.500	2.500	2.500
Uplink	0.750	0.750	0.750	0.750
Downlink	4.460	16.500	16.300	8.300
Payload (camera+FPGAs)	0	5.216	5.216	14.160
Board	0.350	0.350	0.350	0.350
Thermal control	0	0	0	0
Propulsion	0	0	0	0
Mechanics	0	0	0	0
<b>Total</b>	<b>8.060</b>	<b>25.316</b>	<b>25.116</b>	<b>26.060</b>

frequency) and design activity (percentage of interconnects switching). Generally, high-speed and high-density designs consume more power and hence, generate high-junction temperatures. Consequently, the FPGA power dissipation directly limits the design density, system performance, device stability and packaging options. In the course of a design cycle, power profiling for FPGA devices can be carried out at three distinct phases: concept phase – this involves using the Xilinx power estimator (XPE) to give a rough estimate of the FPGA device power based on the estimates of logic capacity and activity (or toggle) rates; design phase – this uses a software tool (XPower Analyser) to give a more accurate FPGA device power based on the detailed information about how the design is implemented in the FPGA; and system integration phase – this involves obtaining the FPGA device power consumption in a laboratory environment using the actual instrumentation. It is a good practice to ensure an accurate power calculation at an early stage in the design cycle to reduce problems later in the actual system integration.

The main goals of estimating power consumption are for power supply equipment sizing and thermal reliability evaluation. In this research, the FPGA power estimation is performed at the concept phase of the design cycle. This is supported by an experimental arrangement to measure the actual power consumption of the FPGA device in a typical digital design implementation. At any time during the design cycle, the XPE can perform a power analysis. The Xilinx power estimator (XPE) utilises the amount of logic in the design and the configuration data to estimate power consumption. The power estimate is as closely as possible to the value obtained at the system integration phase. The XPE tool comprises spreadsheets for entering in the design data (such as device type, clock, logic, I/O, block RAMs, DSP) and obtaining the power estimates based on the device utilisation for the application. Thus, accurate estimates are obtained based on the accurate input values of the clock rates, resource utilisation and activity (or toggle) rates. The power estimation procedure can be summarised as follows: Specify

the target device-package-grade combination; Estimate the expected design resources; State the clock frequency(ies); Estimate the FPGA design's data toggle rates; Specify the design's external storage and transceiver interfaces and data rates; and State the FPGA's operating thermal environment.

In this paper, the target device-package-grade combination is XC3S500E-FT256-commercial. The clock frequencies for the case study digital design(s) for the CubeSat's meteorological mission are 50 MHz (default onboard clock) and 100 MHz (derived clock). The average toggle rate of the signals in the system logic and data for the FPGA design is chosen as 12.5 %; this assumes that at least 1/8th of the I/O signals toggle at each clock cycle and is a default value for this device. The I/O standard for the FPGA device (based on the datasheet published by Xilinx) is LVCMOS 2.5 V, 8 mA (slow). The ambient temperature of the environment in which the FPGA will be operating is 25°C; this fixes the operating junction temperature of the device at 28.5°C. The XPE tool was utilised to calculate the FPGA power consumption of a Xilinx Spartan-3E device at the conceptual design phase. Moreover, to investigate the power consumption of the FPGA device during a typical practical implementation, a measurement system was designed. The experimental setup for an FPGA-based application is explained later in this section.

To study the FPGA power consumption onboard a small satellite (e.g., CubeSat) system, an image processing application was considered. For a CubeSat's Earth observation mission (EOM), data capturing, processing and transmission to a ground station (in both real-time and non-real-time) would require an appreciable amount of electrical power. Direct transmissions of raw satellite data require a substantial amount of communication bandwidth, downlink time slots and transmitter power. Hence, an onboard data processing using digital signal processing (DSP) devices such as FPGAs is recommended. Deploying FPGAs on the satellite payload module (such as imagers) for a large amount of data to be transferred between the FPGA target and the onboard computer (OBC) would reduce the system power requirement and

enhance the mission capability. An onboard data processing can reduce the data (image) quality and this depends on the compression algorithm (such as JPEG and PNG) and the threshold ratio utilised. The benefits of onboard data processing include the reduction in the transmitter power and transmission slots/communication bandwidth requirements.

Direct memory access (DMA) (FPGA module) is a first-in-first-out (FIFO)-based method of transferring data between the FPGA target and the host OBC. Other data transfer methods for communicating between a FPGA virtual instrument (VI) and a host VI programmatically include programmatic front panel communication (FPGA module) and user-defined I/O variables (FPGA module). Programmatic front panel communication is used for small, frequent data transfers while user-defined I/O variables transfer coherent sets of FPGA I/O data to and from a real-time host VI. However, DMA is the fastest method of transferring large image data within and from a satellite system since it does not involve the host OBC processor. Thus, DMA communication frees the OBC processor to perform other functions (including calculations) during data transfer. It saves FPGA resources when transferring arrays of data and automatically synchronises data transfer between the OBC and the FPGA target. Typical satellite applications involve data streaming, transferring waveform data between the FPGA target and the OBC; transferring large sets of data; data logging; and running algorithms efficiently (such as manipulating signals from multiple input channels).

An image processing application involving a host VI and a FPGA target is illustrated in Fig. 13. The top-level host VI is shown with the capability to read/write and display images and obtain the pixel arrays information for processing. It has an input image control function which specifies the path to the image to be processed – and this can be a real-time or an off-line image processing. The case study image is a portable network graphics (PNG) image format of the Globe (Earth). The information about the image is obtained using the Read PNG File sub-VI; the image data shows that the image depth is 32 bits per pixel and the image resolution is 225 x 224. The first image processing involves obtaining an image cluster from a reverse 1-D array process. The image cluster resulting from the processed version of the image is fed to the Write PNG File sub-VI which stores the output in the appropriate memory space/file directory. The Read/Write control function in a host VI can be utilised to access the front panel controls and indicators of the FPGA VI. Globe is the original image while Globe 2 is the 1-D processed image. Furthermore, a 2-D image processing can be carried out using the Unflatten Pixmap sub-VI and a convolution block. The data type of the 2-D array is changed to Double and convolved with a convolution mask typically used for edge detection. A constant offset amounting to the value of the midpoint between 0 and 255 is added to the 2-D array output of the convolution block. With the Unflatten Pixmap sub-VI, the image depth can be varied depending on the desired image quality. The host VI control of the FPGA target is achieved using the Open FPGA VI Reference, Read/Write control function and the Close FPGA VI Reference. Globe 3 is the final 2-D processed image. As indicated before, the desired image depth for the processed image can be manipulated for the purpose of data transmission; for instance, Globe 3 image is a 24-bit pixmap of the original 32-bit per pixel Globe image.

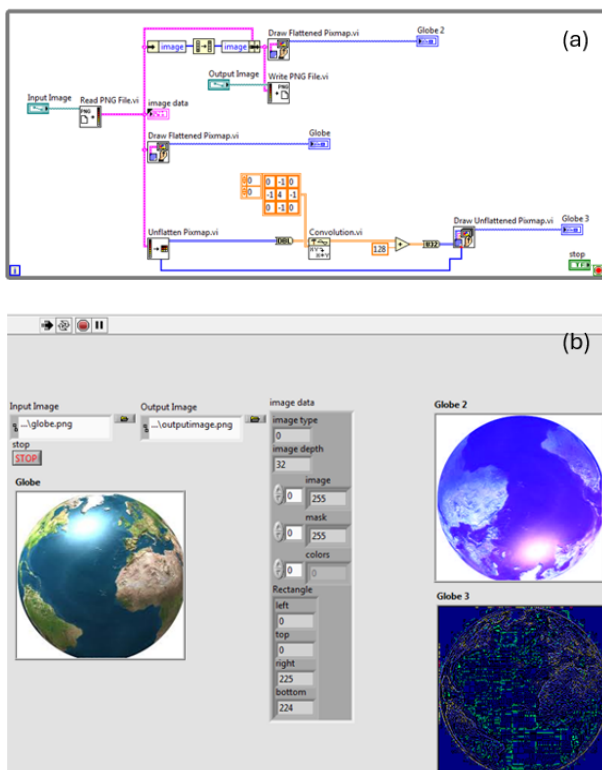


**FIGURE 13.** An Image Processing Application for a Host VI-FPGA Target Implementation, (a) Block diagram and (b) Front panel

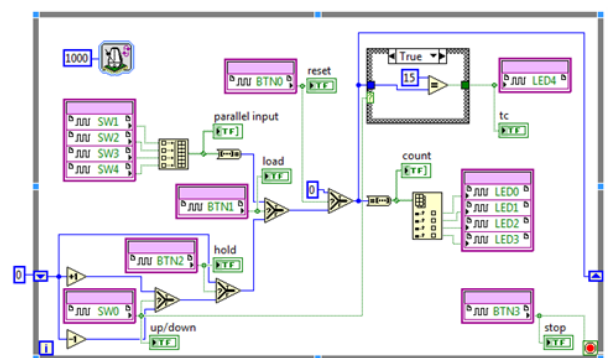


**FIGURE 14.** A Programmable Counter Circuit

The graphical programming code (Fig. 13(a)) can be implemented on the host PC (or CubeSat's OBC). However, the data transfer speed is highly dependent upon the host processor's speed and availability. The NI DE FPGA board does not support the aforementioned data transfer methods for image

processing applications. Hence, a supported FPGA-based application was developed to illustrate the basic power regimes of the FPGA for an adaptive CubeSat system engineering analysis. The digital design implemented on the FPGA is shown in Fig. 14. The application is a 4-bit programmable counter which is capable of: up- and down-counting; resetting; providing terminal count indication; loading a parallel 4-bit input; and holding a count based on the required function through input signals.

A SRAM FPGA device (Xilinx SPARTAN XC3S500E-4FTG256C) was chosen to examine the FPGA power components. The goals of the power estimation were to enhance the development of a reliable power/energy budget model for small satellites (e.g., CubeSat) and to critically examine the literature report on SRAM-based FPGA devices and hence, justify the choice of the flash FPGA technology for the HASS architecture. The experimental setup consists of a National Instrument (NI) digital electronics FPGA prototyping board, ELVIS II prototyping board, power adapters, computer system (running the LabVIEW (LV) FPGA and XPE softwares), visual display unit (VDU)/monitor, flex wires and USB cables. The CubeSat-scaled FPGA project was implemented using the LabVIEW FPGA. The developed top-level FPGA/LV-virtual instrument (VI) code was downloaded onto the FPGA target (DE FPGA Board) for compilation and subsequent implementation. The compilation tool was Xilinx 12.4. Following the successful completion of the compilation, the estimated (pre-synthesis and synthesis) and final (map) device utilisations were obtained.

The FPGA compilation data were used to estimate the power consumption of the device at 50 MHz and 100 MHz. At the onboard clock frequency of 50 MHz, the device utilisation for the digital counter application includes 656 slice FFs and 676 slice (4-input) LUTs. Similarly, at 100 MHz, the device utilisation comprises 721 slice FFs and 744 slice (4-input) LUTs. The system data module of the FPGA device uses a single data rate (SDR) with 15 input pins and 29 output pins based on the report of the programmable counter compilation. The results of the power profiling and thermal modelling at 50 MHz (Fig. 15) and 100 MHz (Fig. 16) are presented in this paper. It is obvious from the plots that the quiescent (static) power consumption of the FPGA device at clock frequencies of 50 MHz and 100 MHz are 78 mW and 79 mW respectively. The total power consumptions of the FPGA device at 50 MHz and 100 MHz clock frequencies are approximately 115 mW and 139 mW respectively. Hence, an increase in the switching frequency results in a significant increase in the dynamic power consumption of the FPGA device. This is further supported by the presented power and thermal profiles. In more complex designs, the combined power consumption of the functional blocks would be higher than the static (device and design) power consumption. Moreover, the FPGA power modelling accounts for the system temperature and voltage sensitivity. The power dissipation at ambient temperature is 11 mW at 50 MHz whereas the 100-MHz switching frequency consumes 14 mW. Moreover, as the switching frequency

increases, the power dissipation of the FPGA increases; this is more obvious in the dynamic power consumption of the FPGA device for the same application.

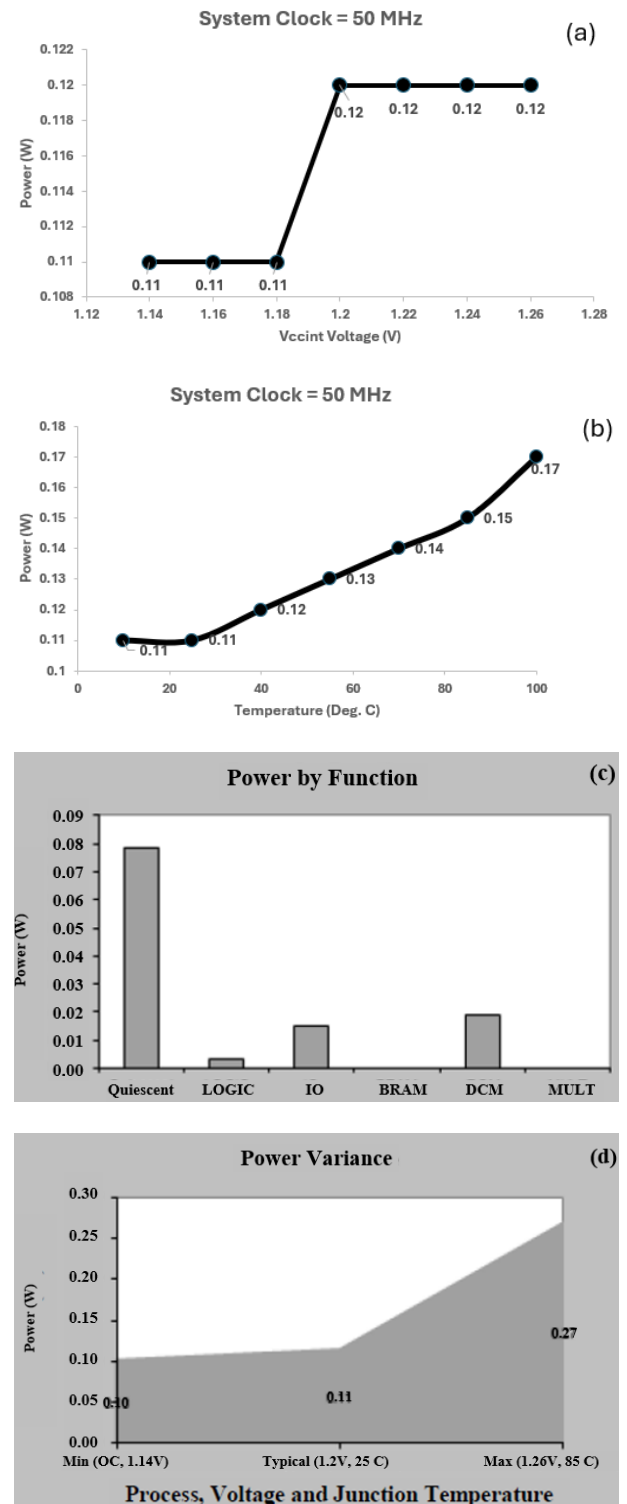


**FIGURE 15.** Power Consumption Profiles of XC3S500E (System Clock = 50 MHz): (a) Power versus Voltage; (b) Power versus Temperature; (c) Power by Function and (d) Power Variance

**TABLE 7. Average power consumption of the FPGA resources**

Measurement Procedure	Connected Device	Average Power Consumption (W)	Average Power Consumption per Device/Implementation Mode (W)
Step 1	Power supply module (PSM)	0.15	0.15
Step 2	PSM + NI ELVIS II power supply adapter	3.35	3.20
Step 3	PSM + NI ELVIS II power supply adapter + NI ELVIS II board (prototyping board switch is "Off")	14.10	10.75
Step 4	PSM + NI ELVIS II power supply adapter + NI ELVIS II board + NI DE FPGA board (DEFB switch is "Off")	15.50	1.40
Step 5	PSM + NI ELVIS II power supply adapter + NI ELVIS II board + NI DE FPGA board (DEFB switch is "On"); pre-compilation mode	16.25	0.75
Step 6	Compilation mode*	16.25	0
Step 7	Static (Post-compilation) mode	16.30	0.05
Step 8	Dynamic mode	16.35	0.05

Application: A Programmable Counter targeting the NI Digital Electronic FPGA Board.

Equipment: 1 No. NI DE FPGA board; Host PC, NI ELVIS II board; 1 No. power supply adapter; 2 Nos.

USB cables; 1 No. Power meter (PX 120 after Matrix, 600 V CAT III); 1 No. Power supply module

Table 7 shows the measured results of the power consumption for the programmable counter application ( Fig. 14). This was executed on the Xilinx Spartan-3E FPGA device that is mounted on the NI digital electronics FPGA board. Eight steps were followed in order to accomplish the power measurement. The measurement system calibration and procedure are stated alongside the connected devices. Table 7 gives the order of device connection and the corresponding power consumption measurement. The average power consumptions of the integrated devices and each added device are presented. The sensitivity of the PX 120 meter utilised for the FPGA power consumption measurement was limited to the tenth of a watt. Hence, more advanced power meters with a sub-mW measurement capability would be able to detect small changes in the power consumptions of the various devices especially the FPGA at each stage of the application implementation. For the presented programmable counter, the measured static and total power consumptions are approximately 50 mW and 100 mW respectively. This indicates that the dynamic power consumption approximates the static power consumption for the case study programmable counter application. The measured total power consumption of the FPGA device is less than the XPE tool value by 17 %; it shows a good agreement for a conceptual CubeSat's electrical power subsystem design consideration. Hence, this serves as a critical design consideration for the spacecraft system engineer in terms of power and cooling specifications for the FPGA design and/or application. The NI DE FPGA board consumed approximately 750 mW when connected without downloading any digital code onto it (i.e., pre-compilation state). Since power is a premium space resource, energy budgeting must be performed as an integral part of the satellite system engineering spanning the different design cycles of the subsystems and subsystems of the spacecraft.

The complete FPGA power consumption measurement setup is presented in Fig. 17. The electrical circuit diagram for the FPGA power measurement setup is presented in Fig. 18. The NI DE FPGA board (load) and the PX 120 power meter are connected to the single-phase mains supply via a power supply module. The PX 120 power meter tracks every power consumption change that occurs as the connected devices are switched-on in a step-by-step fashion. Steps 1 to 5 serve to characterise the measurement equipment for the FPGA power consumption measurement. The detailed measurement procedure and devices per measurement step are shown in Table 7. The experimental and analytical power estimation procedures enable a spacecraft system engineer to ensure an appropriate power and thermal budgeting for a given space mission. The estimated power consumption and junction temperature of the FPGA device enables an objective mission evaluation to be carried out for FPGA-based highly adaptive space systems.

An energy reserve budget analysis for adaptive space systems has been carried out. This paper involves an experimental validation of the power consumption of CubeSats with an integrated FPGA. The power generation and payload capabilities of CubeSats are generally limited by their size and weight restrictions. For instance, the one-unit (1U) CubeSat (1 kg and 10 x 10 x 10 cm) can only generate a maximum power of 5.7 W using four solar panels. Similarly, the two-unit (2U) CubeSat (2 kg and 10 x 10 x 20 cm) and three-unit (3U) CubeSat (3 kg and 10 x 10 x 30 cm) can only generate a maximum power of 7.96 W and 10.22 W respectively using four solar panels. Hence, these categories of nanosatellites can only accomplish mission capabilities permitted by their respective power budget margins. The dynamic power regime consumes approximately twice the static power value. These findings demonstrate the need for a careful power budget analysis of FPGA-based small satellite architectures. A 1-

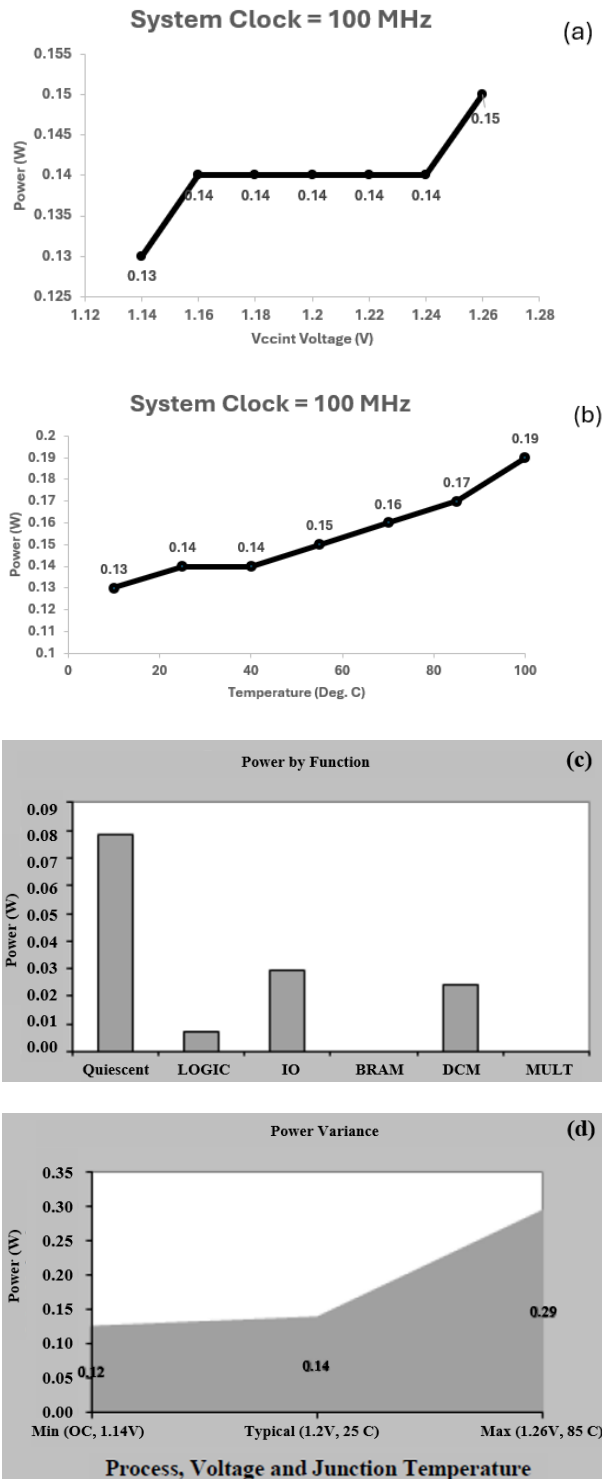


**FIGURE 16.** Power Profiles of XC3S500E (System Clock = 100 MHz): (a) Power versus Voltage; (b) Power versus Temperature; (c) Power by Function and (d) Power Variance

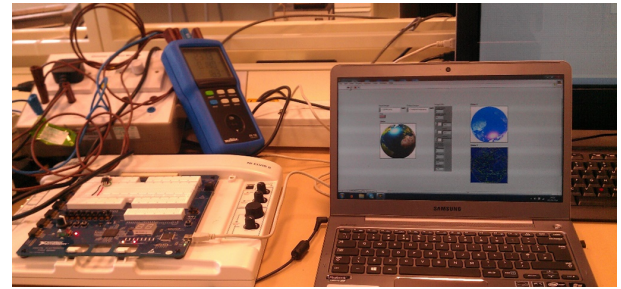


**FIGURE 17.** A FPGA Power Consumption Measurement Setup

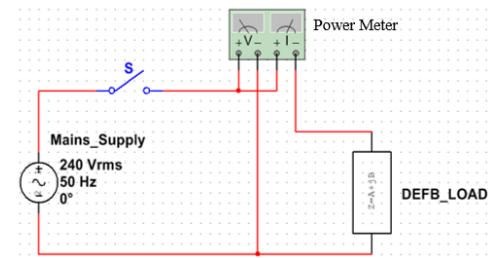


**FIGURE 18.** Electrical Circuit Diagram for a FPGA Power Measurement Setup

of scheduling the HASS (CubeSat)'s payload and core bus subsystems to meet the maximum power supply capability of the solar array and the storage batteries. The CubeSat (or highly adaptive nanosatellite) can accomplish uplink and downlink communications during its communication-overpower power mode. Primary and secondary payloads can also be supported during its data processing-overpower power modes; the payloads would comprise a CMOS camera and low-power radiation-hardened Xilinx Spartan-3 FPGAs. This would result in a reservation of 1575 mW of power for any contingency that might ensue during the CubeSat mission. Moreover, a 3-kg highly adaptive CubeSat (HAC) can enable advanced mission capabilities using radiation-hardened low-power Xilinx Spartan-3 devices and support at least three processing-overpower power modes.

Figs. 19 and 20 show the power analysis plots for the CubeSat's meteorological mission. The total system-level power of the METSAT increases with the subsystem power consumption according to (11). Operating the devices at low power levels implies designing and developing applications codes that would utilise less digital blocks for its process execution. It is evident that the METSAT can be reused for space missions that would require beginning-of-life powers spanning 3 W to 6 W. This is possible by using the HASS architecture and adaptive multifunctional structural unit (AMSU) building blocks for the small satellite system design. It is obvious from Figs. 19 (BoL analysis) and 20 (end-of-life (EoL) analysis) that the 10-year power consumption of the METSAT scales well with the HAC architecture due to its adaptive and efficient power management platform.

The proposed multi-mode multi-source EPS design can

kg CubeSat system performing an Earth-imaging mission with a passive magnetic control for the ADCS can support communication, data processing and energy-storing power modes. The spacecraft system engineer would have the task

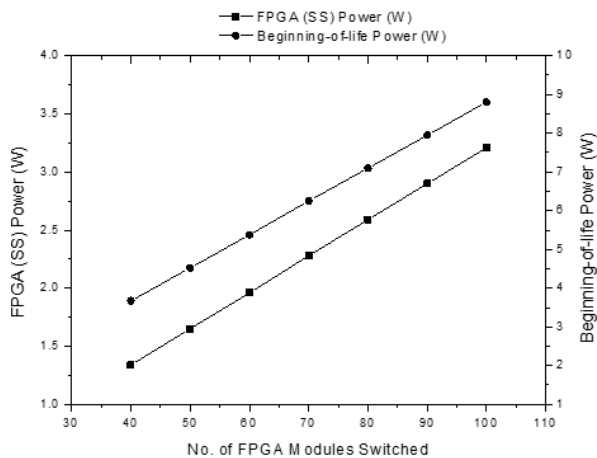


FIGURE 19. A System-level power for a METSAT Mission

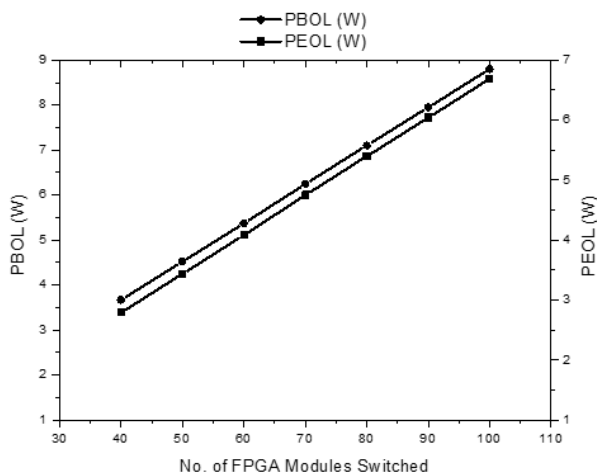


FIGURE 20. A Power Budget for a 10-year METSAT Mission

utilize an additively manufacturing (AM) process to flexibly manufacture and/or remanufacture 3D-printed multi-sourced MIMO multiband RF-PPV energy harvester for ultra-sensitive low-latency CubeSat-Drone-based Earth observation (Fig. 21). The MIMO architecture enables the proposed innovation to achieve a RF-DC energy conversion efficiency of 78% [13]. With a PPV efficiency of 28.6 %, parallel operation and total load-sharing ratio of RF:PPV = 0.7:0.3, additive manufacturing enables the 3D-printed hybrid green energy harvester to achieve a combined system-wide efficiency of 63% [i.e.,  $(0.78 \times 0.7) + (0.286 \times 0.3)$ ] with a daytime power boost. The current state-of-the-art achieves a RF-DC conversion efficiency of up to 75% with no on-demand daytime power boost [13]. The proposed RF-PPV energy harvester will utilise space-grade Gallium Nitride (GaN) transistor technology to conduct optimal voltages over time. GaN has a smaller form factor, is more radiation-hardened and more efficient at transferring current (i.e., less energy is lost to heat, and more energy will charge the CubeSat-IoTs) than sil-

icon devices. With a higher switching frequency, GaN semiconductors enable a quicker wireless power transfer though silicon typically costs less. However, with an improved efficiency of GaN charges, filters, heatsinks, and other circuit components are drastically reduced to achieve cost savings of up to 20%. The Programmable Power Supply standard can be implemented as an advanced charging technology for USB-C devices on CubeSats to enable chargers and devices to interact with one other for a deterministic optimal charging energy.

The current leading conventional wireless RF energy harvesting products do not utilise additive manufacturing and/or remanufacturing to achieve stabilised system-wide efficiency during energy harvesting and during on-demand utilisation. The modelled MIMO multiband RF-PPV energy harvester printed circuit board product achieves a FR4-equivalent performance metrics at sub-6 GHz and mmWave 5G/Wi-Fi frequencies [13]. AM enables the proposed MIMO multiband RF-PPV energy harvester product to (i) have greater flexibility for system-wide efficiency and performance; (ii) perform better than machined surfaces; (iii) reduce the costs and weight of RF components (including antenna and transceiver frontends subsystems); (iv) reduce the fabrication time of RF components (including antennas).

#### IV. GREEN 5G/6G DRONE-CUBE-SAT FOR EARTH OBSERVATION APPLICATION

The proposed Green Drone-CubeSat-Ground station system architecture will enable complementary and supplementary Earth observation services within an artificial intelligence-based 5G/6G space-terrestrial convergence network ecosystem (Fig. 21) [16], [52], [53]. A key sector to benefit from this is the low-altitude economy. For instance, the innovative LEO-based low-latency, high-quality-and-gain (30 dB over the MEOSats) communication throughput CubeSat-IoTs [52], [53] can seamlessly integrate with and enhance the performance of the EU's two civil-controlled satellite navigation systems, viz: (i) Galileo; and (ii) European geostationary navigation overlay service (EGNOS). This can create innovative cutting-edge and disruptive Earth observation solutions in partnership with the private and the public sectors that will benefit the public and the federated continental and/or global satellite telecoms industry. Consequently, ongoing LEO missions (e.g., Copernicus Sentinel-1) can be enhanced to provide four exclusive imaging modes with different resolutions ( $<5$  m) and coverage (beyond 400 km). The measurement data would span multi-purpose imagery (land and sea) and landscape topography.

Wireless power transfer systems in converged 5G/6G TN-NTN will enable interoperable, compatible and affordable wireless device charging to foster research, innovation, and economic growth. The Third Generation Partnership Project (3GPP) is an international standards organization that developed communication standards for the existing and the past generations of radio access technologies (including 3G, 4G and 5G). To accommodate the specific operational and functional autonomy needs of low-complexity, small size, low-

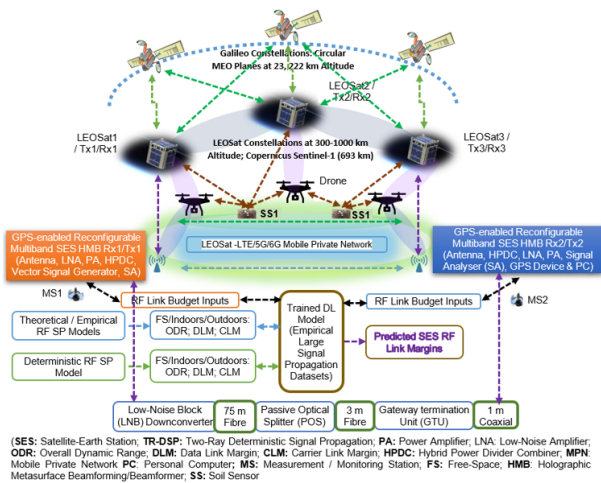


**FIGURE 21. Green 5G/6G Drone-CubeSat for Earth Observation System Architecture**

power, and small weight transceivers, the 3GPP has recognised the “Ambient IoT” devices in the releases TR22.840 and TR38.848 [55]. These small form factor low-power IoTs devices may be batteryless and require below 10 mW. For our reported 650-mW MIMO RF ETH, at least 65 sensors would operate passively, and be carbon neutral-certified wirelessly, and RF-powered operationally. The “3GPP Ambient IoT” (standard Release 19) covers the spectrum allocation, connectivity architectures, coverage use cases, and energy harvesting. A high reliability is required for space-borne equipment due to the prohibitive cost of in-orbit maintenance and the returns-on-investment (ROI) expected. Hence, this paper targets the problem of validating the behavior and electrical power consumption of the CubeSat-IoT’s electronic peripherals to enable the integration of communication, sensing, control, propulsion, beamforming, multiple input multiple output (MIMO) RF architecture frontend and processing components into a final space-grade small satellite system. To obtain a space-borne equipment with a desired reliability and quality, the unit pass reliability and quality values of its constituent components must be qualified respecting the power consumption as a critical premium in-orbit resource for a holistic seamless and ubiquitous TN-NTN connectivity ecosystem.

Since the RF-PPV model will utilise CubeSat-IoTs clusters with energy transmission and harvesting capabilities, long-term energy sufficiency and autonomy will be achieved through at least four operational modes, viz: (i) hybrid RF-solar energy harvesting only; (ii) solar energy harvesting only; (iii) direct RF energy harvesting only; and (iv) ambient (indirect) RF energy harvesting only. The CubeSat-IoTs clusters and/or constellations will adopt a hierarchical multi-tier capacity-based layered architecture to create a generator(s)-user(s) network. For instance, highly adaptive microsattellites (HAMs) will be able to power a cluster(s) of highly adaptive nanosatellites (HANs); HANs will power a cluster of highly adaptive picosatellites (HAPs); HAPs will recharge a cluster

of highly adaptive femtosatellites (HAFs); and HAMs will beam free-space RF-solar energy to clusters and/or constellations of HANs, HAPs, and HAFs. This translates into at least 86% environmental impact reduction (including less waste of materials, energy consumption, manufacturing tooling, and hazardous substances; simplified supply chain; reduced transport footprint; 70% weight reduction; and digital manufacturing-enabled converged space-terrestrial circular economy).

Furthermore, the promising commercial benefits of the WPT technology implies that quality assurance and compliance testing standards must be addressed. The TN segment has a worldwide coalition of businesses that develop standards for wireless RF/microwave/mmWave charging called AirFuel Alliance (AFA). No NTN-based WPT standard for the mMIMO-HetNets has been reported. The AFA has developed a 6.78-MHz [industrial, scientific and medical (ISM)] band standard for charging devices need about 50 W within several distances (cm). AFA’s 900 MHz band (865–868 MHz; and 902–927 MHz) wirelessly charges up to 1 W at several distances (m) [55]. This invocation is promising for autonomous roaming mobile transceivers that are wirelessly powered in the 5G/6G TN-NTN ecosystem. CubeSats-IoTs’ clusters and constellations in space can utilise Bluetooth Low Energy standard to signal between the RF energy transmitter and the receiver. The receiving CubeSats-IoTs can then request power from any transmitter(s) in range. A highly adaptive microsattellite can transmit RF power to highly adaptive nanosatellites, femtosatellites, and picosatellites. The research findings hold a great promise for a real-time seamless ubiquitous 5G/6G MIMO/Wi-Fi 7/8 uplink data throughput versus energy (generation-consumption) balance function profiling within the future-generation converged NTN-NTN ecosystem. A dynamically controlled constant signal-to-noise ratio enables a minimum power transmission for low-cost equipment downsizing and onboard CubeSat battery longevity. This lends credence to the adoption of adaptive multifunctional architectures onboard CubeSats that utilize trajectory data to adapt power transmission to the dynamic radio communication link parameters. An integrated LEO-based terrestrial-non-terrestrial network exhibits dynamic constraints around data traffic, spectrum, power consumption, latency, rural-urban coverage management, and processing capabilities. Our proposed hybrid RF-solar energy harvesting obviates increased power consumption occasioned by higher handover rates for onboard data processing to sustain low-cost RF link profiling and reconfigurable critical and non-critical information transmissions.

The frontal objective of this work is to develop and present experimentally validated estimating CubeSat-IoTs power and relationships that can be utilized to provide reliable and sustainable mission and conceptual system engineering decisions to satisfy performance definitions and budget constraints. This is important because of the increasing dependence on cost-effective, reconfigurable space-borne assets (especially in the low-earth orbit) to complement terrestrial

radio access technologies. The choice of the payload-based power estimating relationship (PER) model for each CubeSat-IoTs mission is informed by the combined statistical analysis of past and current CubeSat-IoTs missions with recourse to the emerging small satellite technologies, duty cycle factors, use cases, and applications. The duty cycle of CubeSat-IoTs payloads represents the percentage of time payloads are active (harvesting energy, and/or transmitting and/or receiving data) compared with the total time (including sleep, passive or idle periods). The duty cycle determines power consumption and thermal conditions management. The operational times of optical payloads are optimised to conductive heat dissipation to the CubeSat-IoT's structure. A balanced duty cycle or operational time ensures a seamless continuous mission activity or allowance for recharging. With balanced data generation and transmission rates, data downlink speed can be reconfigured to control the active duration of the CubeSat payload. A CubeSat-IoT's duty cycle is also heavily influenced by the mission requirements including scientific observations and/or environmental or remote sensing data collection. The proposed power optimization and modes enable the influencing duty or operational cycle to be mission-controlled for mission operation, and/or post-mission reuse successes. The experimental provision in this paper provides a cost-effective validation for a full-scale conceptual design to satisfy any CubeSat-IoT mission objectives realization. 5G/6G MIMO increases data rates, improves signal quality, and enhances energy, and spectral efficiencies in integrated TNs-NTNs to provide a seamless global connectivity ecosystem.

The Green Drone-CubeSat-Ground station system design enables scalable, cost-effective, and high-performing integrated TN-NTN small cells. mMIMO HetNets provide enhanced alternative performance to the conventional mMIMO by reducing the energy consumption per CubeSat-IoTs small cell access point. The presented 3M-ETH algorithm, and system model will enable cost-effective integrated TN-NTN SCAPs to be scaled up to accommodate the prevailing on-demand energy and spectrum traffic. The proposed multi-tier mesh network design will enable the space community to address 5G/6G satellite communication convergence ecosystem use cases and applications for <7 GHz (coverage and spectral efficiency); 7 - 16 GHz (co-existence, coverage and cell density); and 110 - 170 GHz (coverage, energy efficiency, link budget, noise bandwidth, mobility, and co-existence).

## V. CONCLUSION

For a CubeSat's Earth observation mission, data capturing, processing and transmission to a ground station (in both real-time and non-real-time) would require an appreciable amount of electrical power. Direct transmissions of raw satellite data require a substantial amount of communication bandwidth, downlink time slots and transmitter power. This paper presents METCubeSat-IoTs mission payloads with the minimum-to-maximum storable excess energy ratio of 1:3.39. At a Sun-synchronous (polar) 90 orbit, a maximum of 4.81 Wh excess energy storage is achieved. This would

support additional operational times and secondary payloads with two polymer Li-ion batteries (with a combined capacity of 7.78 Wh). Moreover, deploying FPGAs on the satellite payload module (such as imagers) for a large amount of data to be transferred between the FPGA target and the onboard computer would reduce the system power requirement and enhance the mission capability. The FPGA power modelling accounts for the system temperature and voltage sensitivity. The power dissipation at ambient temperature is 11 mW at 50 MHz whereas the 100-MHz switching frequency consumes 14 mW. Moreover, as the switching frequency increases, the power dissipation of the FPGA increases; this is more obvious in the dynamic power consumption of the FPGA device for the same application. The total power consumptions of the FPGA device at 50 MHz and 100 MHz clock frequencies are approximately 115 mW and 139 mW respectively. Hence, an increase in the switching frequency results in a significant increase in the dynamic power consumption of the FPGA device.

The presented multi-mode RF-Perovskite energy harvesting estimating relationship(s) shows that the operational time of any smart CubeSat-IoTs system's hybrid power mode can be optimally modelled for a cost-effective, sustainable and energy-efficient mission application and/or reuse. This holds a great promise in enabling a reconfigurable Green 5G/6G drone-CubeSat development for ultra-reliable low-latency dynamic spatiotemporal Earth observation applications. Sustainable paired / peer-to-peer energy-harvesting-and-transmitting IoTs devices and 5G/6G/Wi-Fi connectivity infrastructure promises to eliminate the need for long battery life and allows nodes to communicate with the network on-demand.

This paper compellingly contributes a pioneering analysis of the energy-harvesting-and-transmitting broadband wireless 5G/Wi-Fi connectivity for the low-altitude economy (spanning LEO-based small satellites, drones and air taxis). CubeSat-IoTs' sustained mission performance is accommodated in its post-mission reuse and/or system-level reconfiguration occasioned by cost-effective and environmentally friendly intelligent small form factor rechargeable battery; smart charging; emergent mission; and space weather eventuality. With complementary supercapacitor / ultracapacitor banks, shallow discharges and recharges can be scheduled for the CubeSat-IoTs to reduce stress on the battery-supercapacitor hybrid. The coordinated CubeSat-IoTs clusters and/or constellations maintain a threshold RF energy signal strength per peer to trigger a peer-to-peer electrical energy supply crisis rescue (or battery recharging) for mission continuity. This is managed within a carefully designed space-borne virtual proximity network (PN), personal area network (PAN), wireless local area network (WLAN), wireless neighborhood area network (WNAN), and wireless wide area network (WWAN) ecosystem. The core trade-off relates to the direct versus stored harvested RF-PPV energy utilisation which would determine the current operational time(s) and/or the mission use case(s) and/or application(s).

## ACKNOWLEDGMENTS

The authors appreciate the SmOp Cleantech for their great contribution in providing supporting advanced industry-linked engineering expertise and implementation resources.

## REFERENCES

- [1] J. Arifin, "Study of CubeSat systems for IoT," in *Proceedings of the 2021 12th International Renewable Engineering Conference (IREC)*, 2021, pp. 1–3. doi: 10.1109/IREC51415.2021.9427817.
- [2] S. Enahoro, S. C. Ekpo, M. C. Uko, A. Altaf, U. e. H. Ansari, and M. Zafar, "Adaptive Beamforming for mmWave 5G MIMO Antennas," in *2021 IEEE 21st Annual Wireless and Microwave Technology Conference (WAMICON)*, 2021, pp. 1–5. doi:10.1109/WAMICON47156.2021.9443616.
- [3] S. C. Ekpo, B. Adebisi, and A. Wells, "Regulated-element Frost beamformer for vehicular multimedia sound enhancement and noise reduction applications," *IEEE Access*, vol. 5, pp. 27254–27262, 2017. doi: 10.1109/ACCESS.2017.2775707.
- [4] S. Enahoro, S. C. Ekpo, and A. Gibson, "Massive Multiple-Input Multiple-Output Antenna Architecture for Multiband 5G Adaptive Beamforming Applications," in *2022 IEEE 22nd Annual Wireless and Microwave Technology Conference (WAMICON)*, 2022, pp. 1–4. doi:10.1109/WAMICON53991.2022.9786100.
- [5] S. C. Ekpo and D. George, "A system engineering analysis of highly adaptive small satellites," *IEEE Systems Journal*, vol. 7, no. 4, pp. 642–648, Dec. 2013. doi: 10.1109/JSYST.2012.2198138.
- [6] G. Araniti, A. Iera, A. Molinaro, S. Pizzi, and F. Rinaldi, "Opportunistic federation of CubeSat constellations: A game-changing paradigm enabling enhanced IoT services in the sky," *IEEE Internet of Things Journal*, vol. 9, no. 16, pp. 14876–14890, Aug. 15, 2022. doi: 10.1109/JIOT.2021.3115160.
- [7] S. C. Ekpo and D. George, "Reconfigurable Cooperative Intelligent Control Design for Space Missions," *Recent Patents Space Technol.*, vol. 2, no. 1, pp. 2–11, 2012.
- [8] A. Dhariwal, N. Singh, and A. K. Kushwaha, "Structural Analysis of 1U CubeSat Designed for Low Earth Orbit Missions," in *2023 International Conference on IoT, Communication and Automation Technology (ICICAT)*, 2023, pp. 1–5.
- [9] S. C. Ekpo, "A multicriteria optimisation design of SPSE for adaptive LEO satellites missions using the PSI method," in *AIAA SPACE 2013 Conference and Exposition*, 2013, p. 5470. [Online]. Available: <https://doi.org/10.2514/6.2013-5470>
- [10] N. E. Hassinate, A. O. Said, and Z. Guennoun, "Communication Link Budget Estimation between Ground IoT Terminal and Cubesat 3U's SDR," in *2022 IEEE International Conference on Internet of Things and Intelligence Systems (IoT&IS)*, 2022, pp. 172–178.
- [11] S. C. Ekpo and D. George, "A system engineering analysis of highly adaptive small satellites," *IEEE Systems Journal*, vol. 7, no. 4, pp. 642–648, Dec. 2013. doi: 10.1109/JSYST.2012.2198138.
- [12] I. Lau, S. Ekpo, M. Zafar, M. Ijaz, and A. Gibson, "Hybrid mmWave-Li-Fi 5G architecture for reconfigurable variable latency and data rate communications," *IEEE Access*, vol. 11, pp. 42850–42861, 2023. doi: 10.1109/ACCESS.2023.3270777.
- [13] M. Uko, F. Elias, S. Ekpo, D. Saha, S. Ghosh, M. Ijaz, S. Chakraborty, and A. Gibson, "Hybrid Wireless RF-Perovskite Photovoltaic Energy Harvester Design Consideration for Low-Power Internet of Things," in *2023 IEEE-APS Topical Conference on Antennas and Propagation in Wireless Communications (APWC)*, 2023, pp. 173–176, doi: 10.1109/APWC57320.2023.10297436.
- [14] F. Elias, S. Ekpo, S. Alabi, M. Uko, S. Enahoro, M. Ijaz, H. Ji, R. Unnikrishnan, and N. Olasunkanmi, "Design of multi-sourced MIMO multiband hybrid wireless RF-perovskite photovoltaic energy harvesting subsystems for IoT applications in smart cities," *Technologies*, vol. 13, no. 3, Art. no. 92, 2025. doi: 10.3390/technologies13030092.
- [15] F. Elias, S. C. Ekpo, S. Alabi, S. Enahoro, M. Uko, M. Ijaz, H. Ji, R. Unnikrishnan, and N. Olasunkanmi, "Passive massive MIMO hybrid RF-perovskite energy harvesting frontend for LEO satellite applications," in *Proceedings of the 5th Space Passive Component Days (SPCD 2024)*, ESA/ESTEC, Noordwijk, The Netherlands, Oct. 2024, pp. 1–7. [Online]. Available: <https://www.spcd.space/>
- [16] F. Elias, S. C. Ekpo, S. Alabi, D. Saha, S. Chakraborty, S. Ghosh, M. Uko, M. Ijaz, and R. Umar, "Rectifier and reconfigurable impedance-matching network analysis for wireless sub-6 GHz 5G/Wi-Fi 6/6E energy harvester," in *The Second International Adaptive and Sustainable Science, Engineering and Technology Conference (ASSET 2023)*, ser. Signals and Communication Technology, Cham, Switzerland: Springer, 2024, pp. 81–90, doi: 10.1007/978-3-031-53935-0\_8.
- [17] J. C. Skippings, S. C. Ekpo, F. Elias, and A. Gibson, "A reconfigurable load-modulated balanced 9-GHz power amplifier design for radar applications," in *The Second International Adaptive and Sustainable Science, Engineering and Technology Conference (ASSET 2023)*, Cham, Switzerland: Springer Nature Switzerland, 2024, pp. 249–257. doi: 10.1007/978-3-031-53935-0\_24.
- [18] A. A. Shah, "A Software-Defined Networking based Simulation Framework for Internet of Space Things," in *2023 IEEE 97th Vehicular Technology Conference (VTC2023-Spring)*, 2023, pp. 1–4.
- [19] S. C. Ekpo, "Parametric System Engineering Analysis of Capability-Based Small Satellite Missions," *IEEE Systems Journal*, vol. 13, no. 3, pp.3546–3555, Sept. 2019.
- [20] L. Tian, N. Huot, O. Chef, and J. Famaey, "Self-Organising LEO Small Satellite Constellation for 5G MTC and IoT Applications," in *2020 11th International Conference on Network of the Future (NoF)*, 2020, pp.100–104.
- [21] M. Zafar, S. Ekpo, J. George, P. Sheedy, M. Uko, and A. Gibson, "Hybrid Power Divider and Combiner for Passive RFID Tag Wireless Energy Harvesting," *IEEE Access*, vol. 10, pp. 502–515, 2022. doi: 10.1109/ACCESS.2021.3138070.
- [22] L. Huan-Jung, L. Wen-Chi, L. Chao-Yang, A. Lin, and H. Chen, "The Line of Sight Distance Measurement by Drone for CubeSat ADS-B Payload," in *2019 IEEE Eurasia Conference on IOT, Communication and Engineering (ECICE)*, 2019, pp. 546–549.
- [23] S. C. Ekpo and D. George, "Impact of Noise Figure on a Satellite Link Performance," *IEEE Communications Letters*, vol. 15, no. 9, pp. 977–979, Sept. 2011.
- [24] P. I. Parra, S. Montejó-Sánchez, J. A. Fraire, R. D. Souza, and S. Céspedes, "Network Size Estimation for Direct-to-Satellite IoT," *IEEE Internet of Things Journal*, vol. 10, no. 7, pp. 6111–6125, April 2023.
- [25] S. C. Ekpo, B. Adebisi, D. George, R. Kharel, and M. Uko, "System-level multicriteria modelling of payload operational times for communication satellite missions in LEO," *Recent Progress in Space Technology. Formerly Recent Patents Space Technology.*, vol. 4, no. 1, pp. 67–77, Jun. 2014.
- [26] H. N. Al-Anbagi and I. Vertat, "Towards Successful Integration of Small Satellites into the Terrestrial IoT Networks," in *2023 International Conference on Applied Electronics (AE)*, 2023, pp. 1–5.
- [27] S. Ekpo and D. George, "A deterministic multifunctional architecture for highly adaptive small satellites," *International Journal of Satellite Communications Policy and Management*, vol. 1, no. 2–3, pp. 174–194, 2012.
- [28] J. George, M. Uko, S. Ekpo, and F. Elias, "Design of an Elliptically-slotted Patch Antenna for Multi-purpose Wireless Wi-Fi and Biosensing Applications," in *e-Prime – Advances in Electrical Engineering, Electronics and Energy Journal*, vol. 6, pp. 100368, Dec. 2023. doi: 10.1016/j.prime.2023.100368.
- [29] J. A. Fraire, P. Madoery, M. A. Mesbah, O. Iova, and F. Valois, "Simulating LoRa-Based Direct-to-Satellite IoT Networks with FLoRaSaT," in *2022 IEEE 23rd International Symposium on a World of Wireless, Mobile and Multimedia Networks (WoWMoM)*, 2022, pp. 464–470.
- [30] S. C. Ekpo, "Thermal Subsystem Operational Times Analysis for Ubiquitous Small Satellites Relay in LEO," *International Review of Aerospace Engineering Journal*, vol. 11, no. 2, pp. 48–57, April 2018. doi: <https://doi.org/10.15866/irease.v11i2.13663>.
- [31] O. Sowande, F. E. Idachaba, S. C. Ekpo, N. Faruk, N. Karimian, O. Ogunmodimu, A. A. Oloyede, L. A. Olawoyin, and S. A. Abdulkareem, "Design of a 3.8-GHz Microstrip Patch Antenna for Sub-6 GHz 5G Applications," in *Proceedings of the IEEE Nigeria Section 4th International Conference on Disruptive technologies for Sustainable Development*, 2022, pp. 1–5.
- [32] S. Ekpo and D. Kettle, "Mm-wave LNAs design for adaptive small Satellite applications," in *Joint 5th ESA Workshop on Millimetre Wave and 31st ESA Antenna Workshop*, 2009, pp. 843–847.
- [33] S. Udeshi, M. Uko, M. Zafar, A. Altaf, B. Adebisi, and S. Ekpo, "Integrated space-enabled hybrid 5G-V2X communications link modeling," *Advances in Communications Satellite Systems*, vol. 37, pp. 1–17, 2019.
- [34] B. Adebisi, S. Ekpo, A. Sabagh, and A. Wells, "Gain Enhancement of Acoustic Beamforming Arrays in Complex Dynamic Systems," in *Proceedings of the 30th Annual Review of Progress in Applied Computational Electromagnetic*, March 2014, pp. 720–725, <http://www.aces-society.org/>.

- [35] S. Ekpo and D. George, "A System Engineering Consideration for Future-Generations Small Satellites Design," in *Proceedings of the First IEEE European Satellite Telecommunications Conference*, October 2012, pp. 1–4.
- [36] J. George, M. C. Uko, S. C. Ekpo, M. Ijaz, R. Kharel, Q. Wang, and H. Ji, "Design of a Multiband RF Slotted-Antenna for Biosensing Applications," in *Proc., 12th IEEE/IET International Symposium on Communication systems, Networks and Digital Signal Processing Conference*, July 2020, pp. 1–6.
- [37] S. Ekpo and D. George, "4–8 GHz LNA design for an adaptive small Satellite Transponder using InGaAs PHEMT Technology," in *Proc. 11th IEEE Wireless and Microwave Conference*, April 2010, pp. 1–4.
- [38] D. Saha, S. Ghosh, S. C. Ekpo, M. Zafar, and A. Gibson, "Gap-Coupled Resonator Loaded Ultra-Wide Band Filtenna for Frequency-Notching Applications," in *3rd European Conference on Communication Systems*, Vienna, Austria, May 2023, pp. 1–5.
- [39] M. Uko and S. Ekpo, "A 23–28 GHz pHEMT MMIC Low-Noise Amplifier for Satellite-Cellular Convergence Applications," *International Review of Aerospace Engineering Journal*, vol. 14, no. 5, October 2021, pp. 1–10.
- [40] S. C. Ekpo, R. Kharel, and M. Uko, "A Broadband LNA Design in Common-Source Configuration for Reconfigurable Multi-standards Multi-bands Communications," in *Proceedings of the ARMMS RF and Microwave Society Conference*, Thame, UK, Apr. 2018, pp. 1–10.
- [41] O. Sowande, F. Idachaba, S. Ekpo, N. Faruk, M. Uko, and O. Ogunmodimu, "Sub-6 GHz 5G Spectrum for Satellite-Cellular Convergence Broadband Internet Access in Nigeria," *International Review of Aerospace Engineering Journal*, vol. 15, no. 2, pp. 85–96, April 2022.
- [42] S. C. Ekpo and D. George, "A Power Budget Model for Highly Adaptive Small Satellites," *Recent Patents on Space Technology*, vol. 3, no. 2, pp. 118–127, Sept 2013.
- [43] S. Ghosh, S. Chakraborty, D. Saha, S. C. Ekpo, A. Chakraborty, F. Elias, and M. Uko, "Design and Analysis of mm-Wave MIMO SIW Antenna for Multibeam 5G Applications," in *Proceedings of the 2023 IEEE-APS Topical Conference on Antennas and Propagation in Wireless Communications (APWC)*, 2023, pp. 154–159. doi: 10.1109/APWC57320.2023.10297489.
- [44] M. Uko, S. C. Ekpo, S. Enahoro, and F. Elias, "Performance optimization of 5G–satellite integrated networks for IoT applications in smart cities: A two-ray propagation model approach," *Smart Cities*, vol. 7, no. 6, pp. 3895–3913, 2024. doi: 10.3390/smartcities7060150.
- [45] M. Uko and S. Ekpo, "8–12 GHz pHEMT MMIC Low-Noise Amplifier for 5G and Fiber-Integrated Satellite Applications," *International Review of Aerospace Engineering Journal*, vol. 13, no. 3, pp. 99–107, June 2020.
- [46] S. Ekpo, "Receiver G/T Ratio Improvement for Space Communications Missions," in *Proceedings of the ARMMS RF and Microwave Society Conference*, Oxfordshire, UK, 2011, pp. 1–2.
- [47] B. Adebisi, S. Ekpo, A. Sabagh, and A. Wells, "Acoustic noise characterisation in dynamic systems using an embedded measurement platform," in *Proceedings of the 30th Annual Review of Progress in Applied Computational Electromagnetics*, Jacksonville, FL, USA, 2014, pp. 726–731. [Online]. Available: <http://www.aces-society.org/>
- [48] N. Saeed, A. Elzanaty, H. Almorad, H. Dahrouj, T. Y. Al-Naffouri, and M.-S. Alouini, "CubeSat Communications: Recent Advances and Future Challenges," *IEEE Communications Surveys and Tutorials*, vol. 22, no. 3, pp. 1839–1862, third quarter 2020.
- [49] M. Uko, M. Zafar, A. Altaf, S. Udeshi, and S. Ekpo, "Link budget design for integrated 5G-LEO communication applications," in *Advances in Communications Satellite Systems*, vol. 37, 2019, pp. 1–9.
- [50] S. Ekpo and D. George, "An Adaptive Radar Design for Small Satellite Missions," in *Proceedings of the World Congress on Engineering*, vol. II, London, UK, July 2011, pp. 1380–1383.
- [51] U. e. H. Ansari and et al., "5G enabled Mobile Operating Hospital and Emergency Care Service," in *2021 IEEE 21st Annual Wireless and Microwave Technology Conference (WAMICON)*, 2021, pp. 1–6.
- [52] S. Enahoro, S. Ekpo, A. Gibson, K. Chow, H. Ji, and K. Rabie, "Multi-radio frequency antenna for sub-6 ghz 5g carrier and data link margin enhancement," in *The Second International Adaptive and Sustainable Science, Engineering and Technology Conference. ASSET 2023*, ser. Signals and Communication Technology, Cham: Springer, 2024.
- [53] A. Altaf, S. Ekpo, M. Ijaz, A. Gibson, and P. Aen, "Novel techniques for 5g/6g power amplifier operation constraints mitigation for satellite-cellular applications," in *The Second International Adaptive and Sustainable Science, Engineering and Technology Conference (ASSET 2023)*, ser. Signals and Communication Technology, Cham, Switzerland: Springer, 2024.
- [54] K. N. R. S. V. Prasad, E. Hossain, and V. K. Bhargava, "Energy efficiency in massive MIMO-based 5G networks: Opportunities and challenges," in *IEEE Wireless Communications*, vol. 24, no. 3, pp. 86–94, June 2017. DOI: 10.1109/MWC.2016.1500374WC.
- [55] E. N. Eyl, N. Athanasopoulos, D. Raddino, and R. Morsi, "Wireless power transfer: Waveform efficiency, interoperability and technology outlook," in *Microwave Journal*, pp. 4–12, November 2024.



**SUNDAY C. EKPO** (Senior Member, IEEE) obtained the MSc. Degree in Communication Engineering from the University of Manchester, Manchester, U.K. in September 2008 and proceeded for his PhD degree in Electrical and Electronic Engineering at the same institution. He holds a PGC. in Academic Practice; MA. in Higher Education; Chartered Engineer; and Senior Fellow of the Higher Education Academy, UK. Dr Sunday Cookey Ekpo is a Chartered Engineer (CEng) with experience of carrying out world-leading fundamental, use-inspired and applied research projects on sustainable radio communication and satellite systems engineering. He designs reconfigurable / digitally-assisted architectures to achieve ultra-low energy and spectrum-efficient multi-radio multi-coverage / range solutions / internet of things products. Dr Ekpo is a Senior Lecturer in Electrical and Electronic Engineering, Manchester Metropolitan University, UK; leads the Communication and Space Systems Engineering research team. He is a British Council Stakeholder for the Innovation for African Universities Projects and Community of Practice. Dr Ekpo's research work spans 120+ peer-reviewed and refereed technical publications and attracted £1.5m+ grants income. Dr Ekpo is a recipient of the Huawei's Influential Thinkers in Engineering and Technology Recognition 2019, and member of the UK Research and Innovation Talent Panel College; Engineering and Physical Sciences Research Council Peer Review College; Institution of Engineering and Technology, UK; internationally recognised R&D leader in Advanced Manufacturing of Electronics; American Institute of Aeronautics and Astronautics Member of the Association of International Education Administrators, USA; Carbon Literacy Champion for the Electrical and Electronic Engineering program; and Principal Investigator of the Sony's Sensing Solutions University Program.



millimeter-wave, and optical transceivers; internet of things sensors characterization; multi-objective system engineering; and complex systems optimization.

**MFONOBONG C. UKO** (Member, IEEE) received his B.Eng. degree in Electrical/Electronic Engineering from the University of Uyo, Nigeria and his MSc in Communication Engineering from The University of Manchester, UK. He is a post-doctoral research fellow in the Communication Engineering department at the Manchester Metropolitan University, UK. His research interest is adaptive satellite system design; multi-physics design, and modelling of RF, microwave,



6G, microwave and millimeter-wave, RF design and modeling, Internet of Things sensors characterization, and RF transceiver characterization.

**SUNDAY ENAHORO** (Student Member, IEEE) received a B.Eng. degree in electrical/electronic engineering, and M.Sc. in Industrial Communication and Automation from Manchester Metropolitan University, Manchester, U.K., where he is currently pursuing a Ph.D. degree in communication systems engineering (Reconfigurable Multiple-Input Multiple-Output Antenna for Multiband 5G Adaptive Beamforming).. His research interest includes 5G antenna design and modeling for Sub-



Metasurface Rectennas for Ultra-low Power 5G/Wi-Fi 6/6E/7/Hallow Applications. Moreover, he worked as a research assistant to develop premenstrual dysphoric disorder (PMDD) sensors which was funded by the Royal Academy of Engineering. His expertise encompasses RF engineering, including subsystem design, rectifiers, antenna design, and RF transceiver characterization. His research interests lie in metamaterial and metasurface analysis, specifically emphasizing energy harvesting and antenna applications, driving innovation in wireless communication technology. Engr. Fanuel served on the technical programme committee for the Second International Adaptive and Sustainable Science, Engineering and Technology (ASSET) Conference 2023 and as Publicity Chair for the Third ASSET Conference 2024, both held in Manchester, UK.

**FANUEL ELIAS** (Student Member, IEEE) is an accomplished Electrical and Electronics Engineering researcher who received his first-class B.Eng degree in Electrical and Electronics Engineering from the Manchester Metropolitan University, UK, in 2023. His award-winning final year project focused on Reconfigurable Wireless WI-FI6/6E/7/5G Energy Harvesting Design. He is pursuing a PhD in RF Engineering and specializes in Reconfigurable Holographic Multi-Radio



in setting the strategic direction of the business and authority to commit resources to support Research and development projects make him the ideal candidate to act as Senior Business Employee. Mr Alabi was the Technical Programme Chair at the Second International Adaptive and Sustainable Science, Engineering and Technology (ASSET) Conference 2023 held in Manchester, UK and gave Keynote Speeches on "Hybrid Wireless Power Transfer for Passive Electronic Appliances" (ASSET 2023); and "Advanced Manufacturing of Electronics for Green Energy Harvesting Use Cases and Applications" (ASSET 2024). SmOp CleanTech was the Diamond Sponsor of the ASSET Conference and Mr Alabi is an Executive Stakeholder of the ASSET Council. has 10 peer-reviewed and refereed technical publications and 10+ peer-reviewed articles on "green energy development for future-generations telecoms infrastructure" in-preparation. Under Stephen's R&D engineering leadership, SmOp has developed intellectual properties and patentable green radio frequency communication and low-carbon hybrid RF-solar energy harvesting products for different horizontal and vertical use cases spanning civil and commercial applications for the major industries/sectors. He currently leads the R&D of passive, hybrid and active energy-efficient and ultra-low-carbon internet of things sensors electronics innovations using advanced nanoscale integrated manufacturing technology for the global net zero attainment.

**STEPHEN ALABI** is the Founder and Managing Director of SmOp CleanTech and has overall responsibility for its operational performance. Stephen is also the driving force behind SmOp's strategic plan. He holds a BSc in Engineering Physics and a MSc in Advanced Process Design for Energy from The University of Manchester, UK. His background is in the scientific aspects of the Company's project which has aided products delivery and knowledge transfer. Stephen's involvement



**MUHAMMAD IJAZ** (Member, IEEE) has received his M.Sc. in Optoelectronic and Communication Engineering from Northumbria University at Newcastle upon Tyne, UK in 2009. He has been awarded Northumbria University studentship to pursue his PhD and awarded PhD degree in 2013 from Northumbria University, UK for his research work in Free-Space Optical (FSO) Communications. He also worked as Research Fellow in Visible Light Communication/LiFi at University of Edinburgh, UK between 2013-15. Dr Ijaz is currently working as Reader (Associate Prof.) and International Lead at Department of Engineering, Manchester Metropolitan University, UK. He is head of Laser and Optics Communication (LOC) lab from 2017 at the department where he is leading applied research and has been working with a number of industries, technopreneurs, international collaborators and successfully leading knowledge transfer partnership projects funded by Innovate UK in the areas of optical wireless communications, embedded systems, IoT, cloud, communication networks 6G, digital signal processing and smart sensors design and secure more than £900K funding from 2020-2023. He has an exciting publication record (90 in total) with high quality journals mostly in Quartile 1, one book chapter, and high-quality conference papers.



techniques.

**RAHUL UNNIKRISHNAN** received his bachelor's degree in Electronics from University of Calicut and master's degree in Electronics Science from Cochin University of Science and Technology, India in 2016 and 2018 respectively. He is currently working as an RF Electronics Design Engineer/KTP Associate at Manchester Metropolitan University and SmOp Cleantech Ltd., UK. His current research interest includes antennas, RF sensors, beamforming and energy harvesting



**NURUDEEN OLASUNKANMI** is the Research and Development Officer for SmOp Cleantech. He is currently the Company Supervisor on KTP projects for RF Electronics Design and Energy Harvesting, between Manchester Metropolitan University and SmOp Cleantech Ltd., UK. He had his PhD in Applied Physics (Geophysics) and Senior Lecturer in the Department of Physics and Materials Science, Kwara State University, Nigeria.

...